**Feasibility and implications of the Northern Sea Route choice: The role of commodity prices, in-transit inventory, and alternative operational modes for the oil product tanker market**


## Abstract

The feasibility of the Northern Sea Route (NSR) is assessed against the established Suez Canal route (SCR) and the longer Cape of Good Hope route. The analysis reflects real practices of route choice for oil products between the Far East and Europe depending on varying market conditions. A required freight rate (RFR) model is developed based on both optimal speeds and real speeds. Automatic Identification System (AIS) data are used to identify route choice patterns and real speeds of Long Range 2 (LR2) tankers during 2013-2020. Cargo value on-board and alternative fuel types/modes based on oil, and current and future technologies of dual fuel Oil/Liquefied Natural Gas (LNG) are considered. Cape is a competitive alternative under low fuel/commodity prices, and its use is explained, especially during the oil oversupply in 2015-2016 and 2020. The NSR is more competitive when moving towards short-hauls, under high fuel/commodity prices, and discounted or zero icebreaking fees, but is uncompetitive most of the times when ice damage repairs are included in the model.



## Keywords

northern sea route; tanker; fuel types; AIS data; speed optimization; required freight rate; in-transit inventory; commodity prices


## 1. Introduction

The NSR has gained momentum as an alternative to traditional maritime routes since the 2010s owing to the gradual sea ice retreat in the Arctic, especially during the summer and autumn months. The trend towards shrinking Arctic sea ice cover is well documented since 1979, with projections of accessibility on Arctic waters for either ice class ships, that is, ice strengthened ships able to navigate through ice, or non-ice class ships, to increase throughout the 21st century (Smith and Stephenson 2013).

An average of 51% of the exploratory voyages which occurred on the NSR in 2011-2014 involved oil products, followed by a sharp decline to 12% in 2015-2020 (CHNL 2021). High commodity and fuel prices, a rising value of cargo and low commodity futures prices along with a competitive icebreaking tariff policy and Russia's ambitions to promote the NSR resulted in an increased number of exploratory tanker voyages, especially during 2011-2013. A rapid decline in tanker voyages since 2014 is attributed to geopolitical factors, low oil prices, shifts in petroleum flows, lower piracy insurance premiums for Suez Canal transits, and changes in icebreaking fees policy amongst others, as mentioned by a Tanker Company, July 12, 2018, and Theocharis et al. (2019; 2021).

The literature on Arctic shipping for oil tankers has so far focused on the potential cost and time savings that the NSR can provide against the established SCR route (Lasserre 2014; Meng, Zhang, and Xu 2016; Theocharis et al. 2018). However, route choice for energy commodities

depends on market structure as much as it depends on transport costs. Whilst the SCR is the dominant route for oil product cargoes between Asia and Europe, the shorter NSR has been tested as an alternative on the back of high fuel and commodity prices, especially during 2011-2013. Moreover, the longer route via the Cape of Good Hope is used as an alternative to SCR, especially when fuel and commodity prices are very low, such as during 2015-2017 and 2020, when oil oversupply and very high commodity futures prices favoured the delay of arrivals at the destination (Bloomberg 2021; Refinitiv Eikon 2021).

This paper aims to assess the feasibility of the NSR within the wider context of route choice for energy commodities, using the oil product tanker segment as an example. It draws from historic NSR kerosene/gasoil voyages and respective flows on established routes between Asia and Europe using AIS data and considering determining cost and market factors. A RFR analysis is developed, based on both optimal speeds and real speeds to assess the break-even point of competing routes from the shipowner's perspective. The time value of cargo is considered by including in-transit inventory costs in the analysis, based on commodity price levels. On one hand, the NSR is compared as a shorter alternative to the SCR. On the other hand, the longer Cape route is considered as an alternative to both the SCR and NSR to assess how route choice is determined based on varying cost and market factors.

Alternative operational modes, and current and future technologies, including Oil/LNG dual-fuel engine set-ups are considered, drawing from Sovcomflot's dual-fuel Aframax tankers with LNG tank capacity of 1,700 $m^3$, as well as recent orders of dual-fuel LR2 tankers from Shell and Hafnia/BW Group, involving LNG tank capacity of 3,600 $m^3$ (Clarksons 2021). Current and future emissions reductions policies are considered, such as the IMO sulphur limit, a future prohibition on the use of heavy fuels in the Arctic, and the Initial IMO greenhouse gas (GHG) strategy.

The remainder of this paper is organised as follows: The literature review is provided in Section 2. The methodology is presented in Section 3, followed by the analysis in Section 4. A discussion of the findings and conclusions, as well as future research directions are provided in Section 5.

## 2. Literature review

The economic feasibility of the NSR is primarily determined by sea ice conditions, the navigation season, month and zone, variability of ship speed through ice, as well as on the ice class of a ship (Stephenson, Brigham, and Smith 2014; Faury and Cariou 2016; Xu, Yang, and Weng 2018; Faury, Cheaitou, and Givry 2020; Theocharis et al. 2021). The use of the NSR also entails certain premiums, including additional crew, insurance, and capital costs, as well as increased fuel consumption depending on the ice class of a ship and sea ice conditions (Lasserre 2014; Theocharis et al. 2018; Solakivi, Kiiski, and Ojala 2018). Moreover, the factoring of ice damage repairs in voyage economics could render the NSR competitive only under increased distance savings between origin-destinations (Theocharis et al. 2019). Transit tariffs for competing routes can significantly undermine competitiveness, with icebreaking fees found to comprise a large part of NSR voyage costs (Zhao, Hua, and Lin 2016; Xu, Yang, and Weng 2018, Theocharis et al. 2019; Wang et al. 2020). On one hand, official icebreaking fees are determined by the prevailing US Dollar-Russian Rouble (USD/RUB) exchange rates and

reduce the potential of the NSR under high fuel prices due to an inverse relationship between oil prices and the value of Russian Rouble (Shibasaki et al. 2018). On the other hand, a combination of fixed discounted fees and high fuel prices significantly increases the competitiveness of the NSR (Xu, Yang, and Weng 2018; Shibasaki et al. 2018; Theocharis et al. 2019; Wang et al. 2020).

Whilst liner shipping economics dominate the Arctic shipping literature (Lasserre 2014; Meng, Zhang, and Xu 2016; Theocharis et al. 2018), there are a growing number of studies assessing tanker economics from various angles and factors, including economies of scale (Zhang, Meng, and Ng 2016; Theocharis et al. 2019; Wang et al. 2020), fuel price levels and icebreaking fees (Theocharis et al. 2019), the impact of sea ice on voyage economics (Faury and Cariou 2016; Faury, Cheaitou, and Givry 2020; Theocharis et al. 2021), as well as the impact of emissions taxes and regulation (Theocharis et al. 2019; Keltoo and Woo 2020).

Currently, studies investigating the NSR economics in terms of costs and transit times against tanker shipping focus on comparisons with the SCR. Yet, route choice for energy commodities such as oil, refined oil products, and gas, depends on market conditions apart from transport costs. Figure A1 in Appendix A1 shows the number of voyages conducted by LR2 tankers carrying jet fuel/kerosene or gasoil/diesel from Northeast Asia to Northwest Europe between 2013 and 2020. The NSR was used by LR2 tankers for three voyages in 2013 and one voyage in 2018[1]. Although most tankers used the SCR, it is noteworthy that the Cape route was used extensively, especially during 2015-2016 and 2020. Route choice during these periods can be further explained by market structure, where high spot commodity prices but declining futures prices, such as in 2012 and 2013, favour quick transits[2], compared to high commodity futures prices and low spot prices that favour the delay of cargo arrivals at the destination[3] as shown in Figure A2, Appendix A1.

Although alternative fuels, such as LNG, are considered in recent studies concerning liner shipping (Ding et al. 2020; Xu and Yang 2020), the literature on tankers has so far focused on various oil-based fuels (Theocharis et al. 2019; Keltoo and Woo 2020) and current dual-fuel Oil/LNG technologies (Theocharis et al. 2021). Further, the impact of commodity prices is considered in one study (Theocharis et al. 2021), whilst cargo value has been mainly considered in studies concerning general cargo (Wergeland 1992) and liner shipping (Wang et al. 2016), based on article searches in Scopus and Web of Science.

The purposes of this paper are threefold: First, the feasibility of the NSR is assessed against the SCR and Cape routes by taking into account the wider geographical implications of route choice between Europe and Asia for refined oil commodities. Second, a cost model which minimises the RFR against competing routes is developed considering actual route choice depending on cost and market factors. The RFR is assessed under optimal speeds as well as real speeds observed in trade flows between east and west. Third, alternative operational modes and fuel types to address emerging and future emissions reductions policies are considered drawing from current and future technologies. The model considers distance, alternative

[1] Another two LR2 laden voyages were conducted in 2013, but these involved naphtha cargoes from Europe to the Far East (CHNL 2021).
[2] This is known as 'backwardation' and occurs when the price of a commodity trading in the futures market is lower than the spot price.
[3] This is known as 'contango' and occurs when the future price of a commodity is higher than the spot price i.e. the opposite of backwardation.

operational modes and fuel prices, icebreaking fees, commodity prices and the time value of cargo by including in-transit inventory costs.

## 3. Methodology

### *3.1. Modelling approach*

A RFR analysis is developed that determines the break-even cost in US$ per tonne from the shipowner's perspective, considering two modelling approaches. First, speed optimisation is employed to minimise the RFR for a given route alternative. Second, constant speeds are used as opposed to theoretical optimal speeds, drawing from AIS data of LR2 tanker voyages between Northeast Asia and West Europe during 2014-2020. On one hand, the cost per tonne reaches its minimum when speed is optimised with respect to cost and market factors subject to engine technical boundaries. On the other hand, real ship speeds tend to depart from optimal points owing to organisational and technical constraints, ship, and voyage specific variables as well as weather factors (Psaraftis and Kontovas 2013). The two distinct speed regimes are included in the analysis to assess how cost structure and route competitiveness are affected against varying cost and market factors.

#### *3.1.1 Cost assessment and optimal speeds*

The fuel consumption is a function of speed, fuel type heating values, and payload (Psaraftis and Kontovas 2013). The fuel consumption function of an oil-powered tanker using either High Sulphur Fuel Oil (HSFO), Very Low Sulphur Fuel Oil (VLSFO), or Marine Gasoil (MGO) can be expressed as:

$$F_{FO}(s^*, \nabla) = F_{FO\ d} \cdot \left(\frac{s^*_{FO\ L,B}}{S_d}\right)^a \cdot \left(\frac{P+L}{\nabla}\right)^{2/3} \quad (1)$$

Table 1 reports the parameters and variables used in Equations 1-30.

A dual-fuel diesel engine can operate either at gas (LNG) or oil (VLSFO, HSFO, MGO) modes, where each fuel can be used depending on operational choices, market conditions and environmental considerations. The use of LNG also depends on tank capacity constraints that dictate the maximum range of a tanker, beyond which the engine is switched to oil mode. When the engine operates at gas mode, it also uses an oil-based fuel, since LNG requires an ignition source to start the combustion process. Since LNG is also assumed to be used within Emission Control Areas (ECAs), the pilot fuel oil is assumed to be MGO for compliance with ECAs regulations. The exponent $a$ is approximated at three (Psaraftis and Kontovas 2013).

The fuel consumption functions of a dual-fuel tanker that operates at LNG-VLSFO mode can be expressed as:

$$F_{DF\ LNG}(s^*, \nabla) = F_{DF\ LNG\ d} \cdot \left(\frac{s^*_{DF\ LNG\ L,B}}{S_d}\right)^a \cdot \left(\frac{P+L}{\nabla}\right)^{2/3}, \text{ for LNG consumption,} \quad (2)$$

and

$$F_{DF\ Pilot}(s^*, \nabla) = F_{DF\ Pilot\ d} \cdot \left(\frac{s^*_{DF\ LNG\ L,B}}{S_d}\right)^a \cdot \left(\frac{P+L}{\nabla}\right)^{2/3}, \text{ for pilot consumption} \quad (3)$$

Equation 3 follows the same exponential relationship between speed and consumption as in the other fuels. The pilot fuel oil consumption is proportional to the engine speed, which in turn is

nearly proportional to the ship speed. This means that the pilot consumption varies nearly linearly with ship speed (email communication with MAN Energy Solutions, January 2020).

The fuel consumption function when the dual-fuel engine operates at oil mode can be expressed as:

$$F_{DF\,FO}(s^*, \nabla) = F_{DF\,FO\,d} \cdot \left(\frac{s^*_{DF\,FO\,L,B}}{S_d}\right)^a \cdot \left(\frac{P+L}{\nabla}\right)^{2/3} \quad (4)$$

The objective is to minimise the total RFR per voyage of a route alternative (either $RFR_{NSR}$ or $RFR_{SCR}$ or $RFR_{Cape}$):

$$min \sum RFR \quad (5)$$

where $\sum RFR$ denotes the sum of the RFR of all legs of a voyage in either of the three routes.

The $\sum RFR$ of each voyage is a function of fuel consumption at a certain speed (either optimal or constant), distance, total cost inputs and cargo carrying capacity of a tanker for each leg. The RFR model includes in-transit inventory costs (Psaraftis and Kontovas 2013), which are determined by the price of the quantity of jet fuel/gasoil and a relevant interest rate for petroleum products.

Equation 6 presents the RFR function for either HSFO-scrubber or VLSFO modes:

$$RFR = \frac{1}{W} \cdot \left[\left(\frac{D_{SCR,NSR,Cape}}{s^*_{FO\,L,B} \cdot 24}\right) \cdot \left(\left(F_{FO}(s^*_{FO\,L,B}) \cdot P_{FO}\right) + (C_o + C_c + g \cdot C_s) + q \cdot (W \cdot P_C \cdot \frac{r}{365})\right) + C_{TI}\right] \quad (6)$$

whereas equation 7 presents the RFR function for LNG-VLSFO mode, where LNG and pilot MGO (gas mode) are included along with VLSFO (oil mode):

$$RFR = \frac{1}{W} \cdot \left[\left(\frac{D_{SCR,NSR,Cape}}{(s^*_{DF\,LNG\,L,B} + s^*_{DF\,FO\,L,B}) \cdot 24}\right) \cdot \left(b \cdot \left(F_{DF\,LNG}(s^*_{DF\,LNG\,L,B}) \cdot P_{LNG} + F_{DF\,Pilot}(s^*_{DF\,LNG\,L,B}) \cdot P_{FO}\right) + c \cdot \left(F_{DF\,FO}(s^*_{DF\,FO\,L,B}) \cdot P_{FO}\right) + (C_o + C_c) + q \cdot (W \cdot P_C \cdot \frac{r}{365})\right) + C_{TI}\right] \quad (7)$$

Equations 8 and 9 present the RFR for a ballast voyage between the unloading port and repair yard, when ice damage repairs are factored in the model. This RFR includes only fuel, operating, and capital costs.

Equation 8 refers to RFR for oil-based modes (HSFO-Scrubber, VLSFO, MGO). Similar to the RFR for an Asia to Europe voyage, MGO is used along with VLSFO in the VLSFO mode depending on the ECAs mileage, whereas HSFO is scrubbed in the HSFO-scrubber mode.

$$k \cdot RFR = \frac{1}{W} \cdot \left[\left(\frac{D_B}{s^*_{FO\,B} \cdot 24}\right) \cdot \left((F_{FO}(s^*_{FO\,B}) \cdot P_{FO}) + (C_o + C_c + g \cdot C_s)\right) + C_R\right] \quad (8)$$

Equation 9 refers to RFR for LNG-VLSFO mode, using LNG and MGO pilot fuel between the unloading port and repair yard, including within ECAs and non-ECAs legs. LNG and pilot MGO are used in this voyage since fuel consumption requirements satisfy the voyage length,

and LNG is cheaper than VLSFO based on market conditions as of February 2020 (See Section 3.3.).

$$n \cdot RFR = \frac{1}{W} \cdot \left[ \left( \frac{D_B}{s^*_{DF\ LNG\ B} \cdot 24} \right) \cdot \left( \left( F_{DF\ LNG}(s^*_{DF\ LNG\ B}) \cdot P_{LNG} + F_{DF\ Pilot}(s^*_{DF\ LNG\ B}) \cdot P_{FO} \right) + (C_o + C_c) \right) + C_R \right] \quad (9)$$

subject to

$$\underline{S} \leq s^* \leq \overline{S} \quad (10)$$

and

$$b, c, g, q, k, n \in \{0,1\} \quad (11)$$

Table 1. Parameters and variables used in the model.

| **Parameters:** | **Description** |
|---|---|
| $P$ | weight of cargo, fresh water, fuel, lubricating oil, stores, water ballast, crew and effects, and baggage and passengers in metric tonnes (m.t.) |
| $W$ | average weight of cargo in m.t. |
| $\sum_{i=1}^{n} D_{SCR}$ | total SCR distance in nautical miles (n.m.) |
| $\sum_{i=1}^{n} D_{NSR}$ | total NSR distance in n.m. |
| $\sum_{i=1}^{n} D_{Cape}$ | total Cape distance in n.m. |
| $D_{1,SCR}, \dots, D_{n,SCR}$ | SCR distance legs in n.m. |
| $D_{1,NSR}, \dots, D_{n,NSR}$ | NSR distance legs in n.m. |
| $D_{1,Cape}, \dots, D_{n,Cape}$ | Cape distance legs in n.m. |
| $D_B$ | distance for ballast voyage from an unloading port to a repair yard in n.m. |
| $P_{FO}$, $P_{LNG}$ | fuel price in US$ per tonne for fuel oils (HSFO, VLSFO, MGO), and LNG, respectively |
| $P_C, r$ | commodity price in US$ per tonne (here oil products), and interest rate |
| $C_R$ | cost of ice damage repairs in US$ |
| $C_o, C_c$ | operating costs in US$ per day, capital costs in US$ per day |
| $C_{TI}$ | transit costs (canal tolls or icebreaking fees) and insurance premiums in US$ |
| $C_s$ | capital costs of exhaust cleaning systems (scrubber) in US$ per day |
| $s_d$ | design speed in knots |
| $\overline{S}$ | upper speed in knots |
| $\underline{S}$ | lower speed in knots |
| $F_{FO\ d}$ | fuel consumption for oil-based fuels (HSFO, VLSFO, MGO) at design speed in tonnes per day |

| | |
|---|---|
| $F_{DF\ LNG\ d}$, $F_{DF\ Pilot\ d}$ | fuel consumption for LNG and Pilot MGO at design speed in tonnes per day |
| $F_{DF\ FO\ d}$ | fuel consumption for dual-fuel engine when operating on oil-mode (VLSFO) at design speed in tonnes per day |
| $L$ | lightweight of a product tanker in tonnes |
| $\nabla$ | displacement of a product tanker in tonnes |

| **Variables** | **Description** |
|---|---|
| $s^*_{FO\ L,B}$ | laden, ballast optimal speeds for oil powered (HSFO, VLSFO, MGO) engine in knots |
| $s^*_{DF\ LNG\ L,B}$ | laden, ballast optimal speeds for dual-fuel engine (LNG) in knots |
| $s^*_{DF\ FO\ L,B}$ | laden, ballast optimal speed for dual-fuel engine (oil-mode – VLSFO, MGO) in knots |
| $S^*_{FO\ B}$, $S^*_{DF\ LNG\ B}$ | optimal speeds for a ballast voyage to a repair yard in knots for oil powered (HSFO, VLSFO, MGO) and dual-fuel (LNG) engine, respectively |
| $b, c, g, q, k, n$ | binary variables, equal to 1 when dual-fuel LNG mode, dual-fuel fuel oil mode, scrubber, in-transit inventory, and ballast voyages for repairs (oil only, dual-fuel) are considered respectively, and 0 otherwise |
| $\sum_{i=1}^{n} T_{SCR}$ | total SCR transit time in days |
| $\sum_{i=1}^{n} T_{NSR}$ | total NSR transit time in days |
| $\sum_{i=1}^{n} T_{Cape}$ | total Cape transit time in days |
| $T_{1,SCR}, \dots, T_{n,SCR}$ | SCR transit time for each leg in days |
| $T_{1,NSR}, \dots, T_{n,NSR}$ | NSR transit time for each leg in days |
| $T_{1,Cape}, \dots, T_{n,Cape}$ | Cape transit time for each leg in days |
| $T_B$ | transit time for a ballast voyage from an unloading port to a repair yard in days |
| $RFR_{SCR}$, $RFR_{NSR}$, $RFR_{Cape}$ | required freight rate for the SCR, NSR, and Cape routes in US$ per tonne |
| $\Delta RFR$ | RFR differential |

The term $\frac{1}{W}$ transforms $RFR$ to $RFR$ in US$ per tonne, whilst the terms $\left(\frac{D_{SCR,NSR,Cape}}{s^*_{FO\ L,B}\cdot 24}\right)$, $\left(\frac{D_{SCR,NSR,Cape}}{(s^*_{DF\ LNG\ L,B}+s^*_{DF\ FO\ L,B})\cdot 24}\right)$, $\left(\frac{D_B}{s^*_{FO\ B}\cdot 24}\right)$, $\left(\frac{D_B}{s^*_{DF\ LNG\ B}\cdot 24}\right)$ calculate the days at sea for each leg and voyage of the respective fuel type. First order differentiation of Equations (6), (7), (8), and (9) with respect to speeds $s^*_{FO\ L,B}$, $s^*_{DF\ LNG\ L,B}$, $s^*_{DF\ FO\ L,B}$, $s^*_{FO\ B}$, $s^*_{DF\ LNG\ B}$ is carried out to obtain optimal speeds. The partial derivatives are set equal to zero, that is, $\frac{\partial RFR}{\partial_{s^*_{FO\ L,B}}} = 0$, $\frac{\partial RFR}{\partial_{s^*_{DF\ LNG\ L,B}}} = 0$, $\frac{\partial RFR}{\partial_{s^*_{DF\ FO\ L,B}}} = 0$, $\frac{\partial RFR}{\partial_{s^*_{FO\ B}}} = 0$, $\frac{\partial RFR}{\partial_{s^*_{DF\ LNG\ B}}} = 0$, with all optimal speeds subject to lower limit, $\underline{S}$, and upper limit, $\overline{S}$, respectively.

Equations 12, 13, and 14, refer to optimal speeds of oil-powered and dual-fuel gas/oil modes, whilst equations 15 and 16 refer to optimal speeds of ballast voyages to a repair yard, depending on the operational mode.

$$s^*_{FO\ L,B} = \sqrt[a]{\frac{\left((C_o+C_c+g\cdot C_s)+q\cdot\left(W\cdot P_C\cdot\frac{r}{365}\right)\right)\cdot {S_d}^a\cdot\nabla^{2/3}}{(a-1)\cdot(F_{FO\ d}\cdot P_{FO})\cdot(P+L)^{2/3}}} \quad (12)$$

$$s^*_{DF\ LNG\ L,B} = \sqrt[a]{\frac{\left((C_o+C_c)+q\cdot\left(W\cdot P_C\cdot\frac{r}{365}\right)\right)\cdot {S_d}^a\cdot\nabla^{2/3}}{(a-1)\cdot(F_{DF\ LNG\ d}\cdot P_{LNG}+F_{DF\ Pilot\ d}\cdot P_{FO})\cdot(P+L)^{2/3}}} \quad (13)$$

$$s^*_{DF\ FO\ L,B} = \sqrt[a]{\frac{\left((C_o+C_c)+q\cdot\left(W\cdot P_C\cdot\frac{r}{365}\right)\right)\cdot {S_d}^a\cdot\nabla^{2/3}}{(a-1)\cdot(F_{DF\ FO\ d}\cdot P_{FO})\cdot(P+L)^{2/3}}} \quad (14)$$

$$s^*_{FO\ B} = \sqrt[a]{\frac{(C_o+C_c+g\cdot C_s)\cdot {S_d}^a\cdot\nabla^{2/3}}{(a-1)\cdot(F_{FO\ d}\cdot P_{FO})\cdot(P+L)^{2/3}}} \quad (15)$$

$$s^*_{DF\ LNG\ B} = \sqrt[a]{\frac{(C_o+C_c)\cdot {S_d}^a\cdot\nabla^{2/3}}{(a-1)\cdot(F_{DF\ LNG\ d}\cdot P_{LNG}+F_{DF\ Pilot\ d}\cdot P_{FO})\cdot(P+L)^{2/3}}} \quad (16)$$

Equations (6) – (9) are solved by substituting the optimal speeds obtained from Equations (12) – (16) to find the minimum RFR for each leg of a certain voyage.

These optimal speeds depend on fixed costs, including in-transit inventory costs, as well as on fuel prices, and payload. Speeds through ice are assumed to not vary with respect to cost and market factors due to the influence of sea ice on ship speed, and therefore could be determined based on recorded speeds within NSR (Section 3.3.). The second order differentiation results in positive values in all cases, which ensures that the solution is a minimum. Moreover, the solution is unique and is a global minimum (Appendix B1). The only exception is in cases where the speed is constrained, such as on ice legs within NSR or when assuming real, fixed, speeds.

A minimum speed of 5 knots is assumed for an ice class IA tanker as the speed below which it cannot navigate independently, and a maximum speed of 16 knots for all tankers, where the design speed falls between 90-95% of the maximum speed depending on ship size (Theocharis et al. 2019; 2021).

The total distance and time of each leg for a route alternative depends on ECAs zones, fuel types/technologies, fuel tank capacity, range, and commodity and fuel prices. They can be expressed as:

$$\sum_{i=1}^{n} D_{NSR} = D_{1,NSR}+\ldots+D_{n,NSR} \quad (17)$$

$$\sum_{i=1}^{n} T_{NSR} = T_{1,NSR}+\ldots+T_{n,NSR} \quad (18)$$

$$\sum_{i=1}^{n} D_{SCR} = D_{1,SCR}+\ldots+D_{n,SCR} \quad (19)$$

$$\sum_{i=1}^{n} T_{SCR} = T_{1,SCR}+\ldots+T_{n,SCR} \quad (20)$$

$$\sum_{i=1}^{n} D_{Cape} = D_{1,Cape} + \ldots + D_{n,Cape} \quad (21)$$

$$\sum_{i=1}^{n} T_{Cape} = T_{1,Cape} + \ldots + T_{n,Cape} \quad (22)$$

The optimal speed for either operational mode per voyage of a route alternative is defined as:

$$s^*_{FO\ L,B}, s^*_{DF\ LNG\ L,B}, s^*_{DF\ FO\ L,B} = \frac{\sum_{i=1}^{n} D_{NSR}}{\sum_{i=1}^{n} T_{NSR} \cdot 24} \quad (23)$$

$$s^*_{FO\ L,B}, s^*_{DF\ LNG\ L,B}, s^*_{DF\ FO\ L,B} = \frac{\sum_{i=1}^{n} D_{SCR}}{\sum_{i=1}^{n} T_{SCR} \cdot 24} \quad (24)$$

$$s^*_{FO\ L,B}, s^*_{DF\ LNG\ L,B}, s^*_{DF\ FO\ L,B} = \frac{\sum_{i=1}^{n} D_{Cape}}{\sum_{i=1}^{n} T_{Cape} \cdot 24} \quad (25)$$

The optimal speeds concerning ballast voyages from an unloading port to a repair yard are defined as:

$$s^*_{FO\ B} = \frac{D_B}{T_B \cdot 24} \quad (26)$$

$$s^*_{DF\ LNG\ B} = \frac{D_B}{T_B \cdot 24} \quad (27)$$

The RFR differentials between NSR, SCR, and Cape routes are defined as:

$$\Delta RFR = RFR_{SCR} - RFR_{NSR} \quad (28)$$

$$\Delta RFR = RFR_{Cape} - RFR_{NSR} \quad (29)$$

$$\Delta RFR = RFR_{SCR} - RFR_{Cape} \quad (30)$$

Equations (17) – (27) also define non-optimal voyage speeds, and respective distances and times when assuming constant speeds for each route alternative.

This RFR model is consistent with Theocharis et al. (2019; 2021), where distinct voyage legs are defined, and different optimal speeds exist on each leg due to different fuel types and prices, and the non-linear relationship between speed and fuel consumption.

*3.1.2 Cost assessment and real speeds*

Figure 1 depicts the South Korea-UKC annual average voyage speed via SCR, the global average laden LR2 tanker speed, and the theoretical cost minimisation speed without accounting for in-transit inventory. Speed data for the South Korea-UKC LR2 tanker trades are based on 81 unique voyages conducted in 2014-2020, of which 29 were direct voyages of jet fuel/gasoil cargoes of 90,000 tonnes (Bloomberg 2021; Refinitiv Eikon 2021). Global LR2 tanker laden speeds refer to daily speeds in 2014-2020, obtained from Refinitiv Eikon (2021).

Although real average speeds both on the South Korea-UKC route and globally varied depending on freight rates and fuel prices, they have been significantly less responsive than optimal speeds. Actual South Korea-UKC speeds and global LR2 tanker speeds ranged between 11.5-12.8 and 11.8-11.9 knots during 2014-2020, respectively. Similar observations can be made for other Far East-Europe voyages, and for Cape voyages. The average speed between Northeast Asia and UKC was 12 knots between 2014 and 2020, and therefore this

speed is chosen to assess costs for alternative routes versus cost minimisation optimal speeds based on Section 3.1.1.

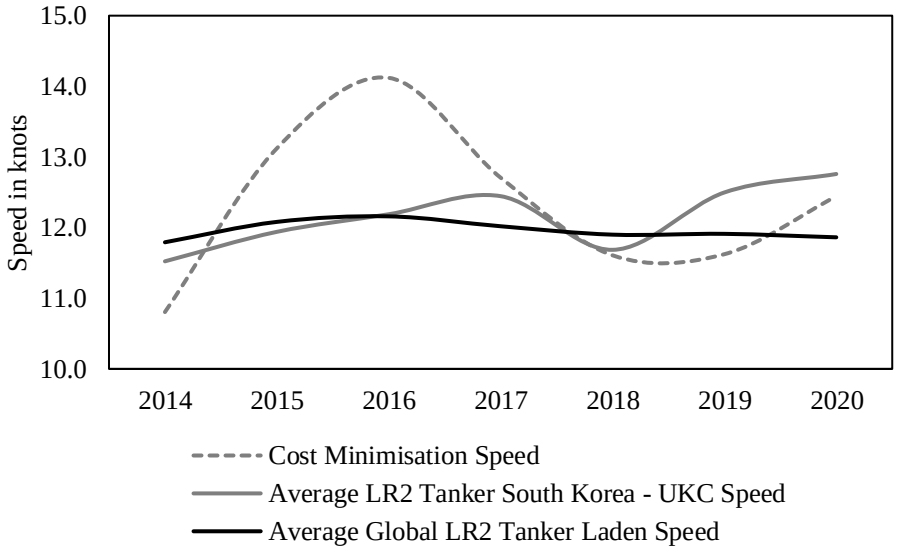


Sources: Refinitiv Eikon (2021), Bloomberg (2021), and Authors' calculations.

Figure 1. Optimal and real speeds of LR2 tanker voyages between South Korea and UKC, and global real speeds during 2014-2020.

### *3.2. Origin – Destinations*

Jet fuel/kerosene and gasoil/diesel comprised on average 63% and 32% of the volume of oil products shipped from Northeast Asia to Europe in 2011-2019 (IEA 2020). Figure A3 in Appendix A1 illustrates the Brent crude oil, and gasoil/diesel and jet fuel/kerosene monthly prices in the major oil hubs of Rotterdam and Singapore during 2011-2020. All products prices correlate with Brent crude price, and all products prices tended to be higher in Rotterdam than Singapore, especially during 2011-2014 and between the second half of 2017 and early 2020. In contrast, products prices converged between the second half of 2014 and 2017, as well as in 2020. This illustrates the typical arbitrage of jet/kerosene and gasoil/diesel, where the West/Northwest Europe region is a large importer of middle distillates from Asia. The biggest importers were the Netherlands, France, the UK, and Spain, whereas the biggest exporters were South Korea and Japan. Three OD pairs are chosen to assess route choice with respect to distance between Northeast Asia and Europe, that is, Ulsan-Bilbao, Ulsan-Rotterdam, and Chiba-Coryton[4]. These reflect the most frequent loading and unloading ports as well as historic port choices for NSR voyages, and LNG bunkering availability (CHNL 2021; Refinitiv Eikon 2021; DNV 2021). Distance savings increase for NSR versus SCR and Cape when moving from the former to the latter OD pair, whereas they decrease for the Cape route versus SCR. Figure 2 illustrates routes, whilst Table 2 presents distances for OD pairs.

Table 2. Origin – Destination (OD) pairs and distances.

[4] An OD pair linking Northeast Asian ports with the UK is chosen instead of France due to proximity of the later with the biggest importer i.e., the Netherlands.

| Origin – Destination (OD) Distance (n.m.) | Northern Sea Route (NSR) | Suez Canal (SCR) | Cape of Good Hope Route | Difference between NSR – SCR | Difference between NSR – Cape | Difference between SCR – Cape |
|---|---|---|---|---|---|---|
| Ulsan – Bilbao | 7,834 | 10,436 | 13,853 | -25% | -43% | -25% |
| Ulsan – Rotterdam | 7,127 | 10,944 | 14,371 | -35% | -50% | -24% |
| Chiba – Coryton | 6,914 | 11,264 | 14,696 | -39% | -53% | -23% |

Source: Dataloy (2021). The distance through NSR is assumed 2,059 n.m. and refers to the deep-water high-latitude route north of the New Siberian Islands, based on the majority of historic NSR voyages (Bloomberg 2021).

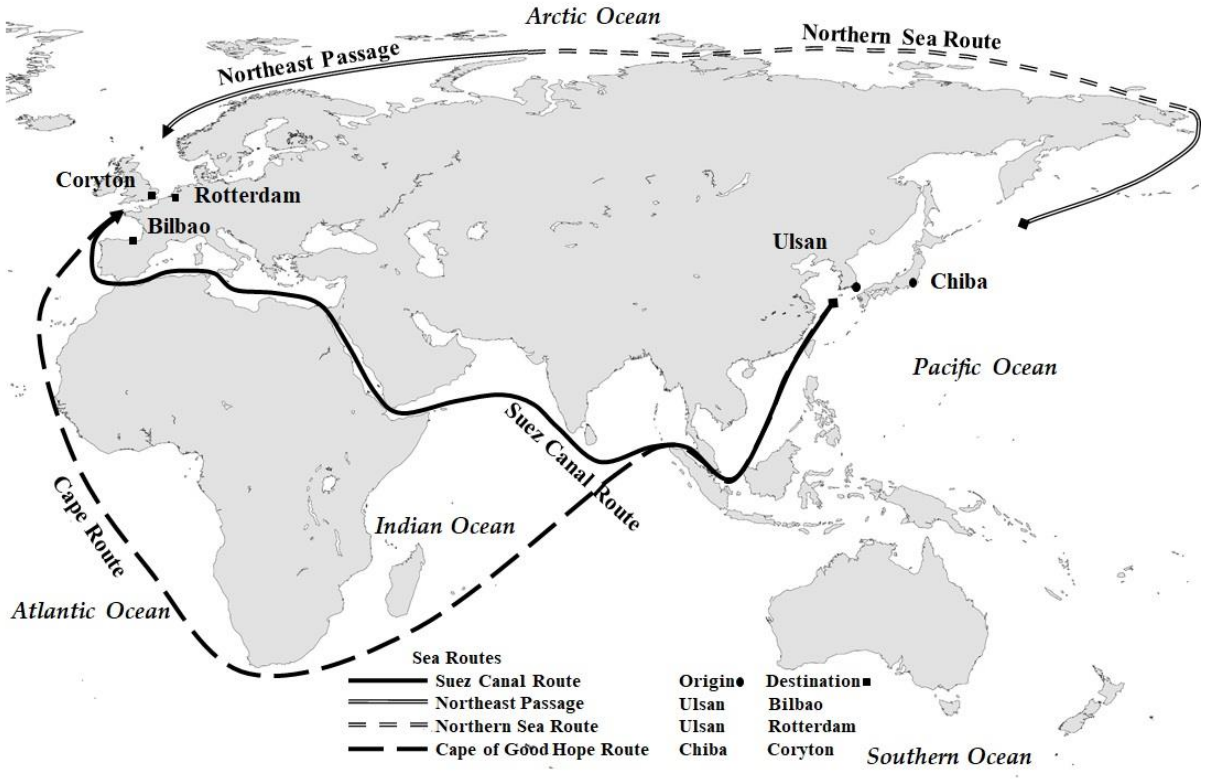


Figure 2. OD pairs and route alternatives (Equirectangular projection map created with NASA GISS G. Projector tool: https://www.giss.nasa.gov/tools/gprojector/)

### *3.3. Costs and operational factors*

The costs and technical factors of Aframax/LR2 tankers, and ice class premiums are presented in Tables 3a and 3b. Table 4 presents the assumptions for fuel and commodity prices. The comparison is based between an ordinary LR2 tanker and an ice class IA (Arc4) LR2 tanker. The ice class IA is in line with the majority of the tankers that used the NSR in 2011-2019 (CHNL 2021). A cargo of 80,000 m.t. is assumed, reflecting average quantities of jet fuel/kerosene and/or gasoil/diesel traded between Northeast Asia and Europe, and conforming to port physical characteristics and LNG bunkering facilities (Appendices C1 and C2).

Table 3a. Costs and technical factors of LR2 tankers of 115,000 dwt, Length Overall (LOA) 250 metres, draught of 15 metres and beam of 44 metres.

| | HSFO-Scrubber | VLSFO | LNG | |
|---|---|---|---|---|
| | | | LNG mode | VLSFO mode |
| Design Speed (knots) [a] | 15 | 15 | 15 | 15 |
| Maximum Speed (knots) | 16 | 16 | 16 | 16 |
| Minimum Speed (knots) | 5 | 5 | 5 | 5 |
| Fuel Consumption (tonnes/day of non-ice/ice class)[b] | 46.7/63.2 | 45.6/61.6 | 36.5/49.6 | 46.7/63.1 |
| MGO Consumption (tonnes/day of non-ice/ice class)[b] | – | 44/59.4 | – | – |
| MGO Pilot Consumption (tonnes/day of non-ice/ice class)[b] | – | – | 0.91/0.98 | – |
| Fuel Tank Capacity (tonnes) [c] | 2,415 | 2,415 | 773 | 1,700 |
| Operating Costs (US$ per day of non-ice/ice class)[d] | 7,974/8,406 | 7,974/8,406 | 7,974/8,406 | 7,974/8,406 |
| Capital Costs (US$ per day of non-ice/ice class)[e] | 13,056/16,861 | 12,296/16,033 | 1,700 $m^3$: 12,827/16,562<br>3,600 $m^3$: 13,736/ 17,912 | 1,700 $m^3$: 12,827/16,562<br>3,600 $m^3$: 13,736/ 17,912 |

Sources: [a]Theocharis et al. (2021), [b]Theocharis et al. (2021), MAN Energy Solutions (2019), email communication with MAN Energy Solutions, April-May 2019 and January 2020, 30.8% higher installed power for IA ice class tanker (Solakivi, Kiiski, and Ojala 2018), [c] Clarksons (2021), [d] average costs for 2011-2018 (Theocharis et al. 2021), [e]average newbuilding prices of LR2 tankers 2013-2019 (Clarksons 2021), average 12-month USD Libor 2011-2019 + 3%, capital recovery factor of 12.5% over 10 years payment (Theocharis et al. 2021), ice class IA premium: 30.4% (Solakivi, Kiiski, and Ojala 2018), ice class IA/B dual fuel premium: 1,700 $m^3$: 4.38%, assuming 30.4% for ice class specification based on Sovcomflot's contracted prices on 2017 compared to ordinary LR2 tankers (Theocharis et al. 2021), 3,600 $m^3$ tank capacity premium: 4.50% based on average newbuilding prices of LR2 tankers of Shell and Hafnia/BW Group (Clarksons 2021), hybrid scrubber (Theocharis et al. 2021).

The LNG-VLSFO mode implies the use of LNG for a certain distance (here, including within the NSR and ECAs zones respectively), depending on the LNG tank capacity, and the use of VLSFO for the rest of the voyage. LNG/VLSFO distance ratios per route and OD pair are presented in Appendix D1. The VLSFO mode implies the use of VLSFO, with MGO used only within ECAs zones. Finally, the HSFO-Scrubber mode allows the use of HSFO for a whole voyage as the scrubber (here hybrid), removes the sulphur of the fuel before it is emitted in the atmosphere. The use of hybrid scrubber is assumed since open-loop scrubbers may be prohibited in certain ports and waterways and/or canals in the future based on assumptions from Theocharis et al. (2021).

Table 3b. Costs, navigational and technical factors.

| | |
|---|---|
| Crew costs[a] | 10% premium in daily crew costs |
| Insurance costs[a] | Ice class premium: US$ 50,000<br>Gulf of Aden piracy premium: US$ 10,500 |
| Ice damage repairs[a] | US$ 180,000; repair yard located in Odense, Baltic region |
| Suez Canal Tolls[b] | US$ 321,539 based on official SCR Toll rates for LR2 tankers, including tugs, mooring, disbursements, pilotage |

| | |
|---|---|
| Icebreaking Fees[c] | Icebreaking fees for 6/7 zones: Low USD/RUB rate of 33.28: US$ 849,238; Base USD/RUB rate of 64.41: US$ 438,793; High USD/RUB rate of 73.7: US$ 383,506<br>Discounted fees: 5 US$/tonne (Lasserre 2014;<br>email communication with Tanker Company, 2020) |
| Transit-related costs[a] | US$ 1,000 per day for ice piloting, pilot travel expenses at US$ 5,000 per voyage, US$ 20,000 for books and charts per voyage |
| Auxiliary fuel consumption[a] | Assumed to be satisfied by the use of the main engine, which depends on the ship and engine set up |
| Port costs, time & cargo handling | Assumed the same for all routes |
| Speed through ice[d] | Average of 10.3 knots, based on the analysis of AIS data of 44 tanker voyages conducted during the summer/autumn seasons of 2011-2019 (Speed range: 5.7-14.4 knots) |

Sources: [a]email communication with Tanker Company (2020), [b]Theocharis et al. (2021), [c]Low USD/RUB rate assumed at high fuel/commodity prices reflecting market conditions between 2011 and 2014, high USD/RUB rate assumed at low fuel/commodity prices reflecting conditions during March-May 2020, base case USD/RUB rate assumed at base case fuel/commodity prices reflecting market conditions before 2020 i.e. 2015-2019 (Bloomberg 2021), [d](Bloomberg 2021).

Table 4. Fuel and commodity prices, and in-transit inventory costs.

| | |
|---|---|
| HSFO Prices[a] | Low: 150 US$/tonne, Base Case: 300 US$/tonne, High: 450 US$/tonne |
| VLSFO Prices[a] | Low: 240 US$/tonne, Base Case: 480 US$/tonne, High: 720 US$/tonne |
| MGO Prices[a] | Low: 250 US$/tonne, Base Case: 500 US$/tonne, High: 750 US$/tonne |
| LNG Prices[b] | Low: 150 US$/tonne, Base Case: 250 US$/tonne, High: 350 US$/tonne |
| Jet/Gasoil Prices[c] | Low: 245 US$/tonne, Base Case: 494 US$/tonne, High: 743 US$/tonne |
| In-transit inventory interest rate[d] | 10% annual rate for oil and petroleum products |
| Notes | Base case oil-based fuel and jet fuel/gasoil price levels as of February 2020 in Singapore and Rotterdam, used as proxies; Low and high price levels assumed at +/- 50% of those at the base case levels, reflecting differences between two distinct periods i.e. average prices during 2011-2014 and during 2015-2017<br><br>LNG prices refer to an average of spot LNG price in Asia and Title Transfer Facility (TTF) gas price in the Netherlands as of February 2020 as proxies, including distribution costs. LNG fuel prices are assumed at +/- 40% owing to a combination of less responsive Dutch TTF and UK National Balancing Point (NBP) gas prices with oil prices, the convergence between spot LNG prices in Asia and crude oil prices during 2011-2014 and 2015-2017, as well as a mix of oil-linked and gas-on-gas competitive pricing regimes in Spain |

Sources: [a](Clarksons 2021), [b]spot LNG prices in Asia (Refinitiv Eikon 2021), TTF gas price in the Netherlands (Theocharis et al. 2021), distribution costs (Theocharis et al. 2021), [c](OPEC 2021), average jet fuel/kerosene and gasoil/diesel spot prices as of February 2020 in Singapore, [d](Theocharis et al. 2021).

## 4. Analysis

### *4.1 Optimal laden and ballast speeds, fuel and commodity prices, and in-transit inventory*

Figure 3 illustrates the relationship between optimal speed and minimum RFR across all route alternatives and fuel and commodity price levels. Results are shown for the Ulsan-Rotterdam pair at the VLSFO mode as an example, given that this is currently the most widely used marine fuel globally. The vertical axis represents the minimum RFR as a function of optimal speed, which is shown in the horizontal axis. Black dotted curves show minimum RFR at optimal laden speeds, whereas grey solid curves show optimal ballast speeds. Black solid curves reflect optimal laden speeds when in-transit inventory costs are included in the model. The figure shows that optimal laden speeds are always lower than optimal ballast speeds across all fuel prices and route alternatives. The reason being higher fuel consumption and resistance when a ship is loaded with cargo than when it navigates in ballast. As a result, the minimum RFR is higher when a ship is laden than when it is not, owing to higher fuel, operating, and capital costs.

The higher the fuel prices, the higher the minimum RFR at the optimal laden than at the ballast speed since the impact of higher fuel prices at the decrease of optimal speed is more pronounced when a ship is loaded than when it is not. Thus, fixed costs are higher at the optimal laden speed, whereas the difference in fuel costs depends on the speed differential at each fuel price level. When including in-transit inventory costs in the model, optimal laden speeds become higher than optimal ballast speeds across all fuel/commodity prices, and route alternatives. This indicates that optimal laden speeds are more sensitive to the value of cargo than to fuel prices, depending on the interest rate, the price of the commodity and its relationship with fuel prices. Not only are minimum RFR rates at laden speeds, including in-transit inventory, higher than those at ballast speeds but also they are higher than those at laden speeds without in-transit inventory. Both fuel and fixed costs are higher at optimal laden than ballast speeds when moving towards higher fuel and commodity price levels. On one hand, a growing value of cargo influences fixed costs more than operating and capital costs per fuel and commodity price level. On the other hand, fuel costs are higher due to both an increased speed differential and increased fuel consumption when a ship is loaded with cargo.

Laden speeds on both SCR and Cape routes are 15.5 knots, 12.3 knots, and 10.7 knots, whereas ballast speeds are 16 knots, 13.6 knots, and 11.9 knots, at low, base case, and high fuel prices, respectively. Laden speeds on the NSR are 13.2 knots, 11.3 knots, and 10.3 knots, whereas ballast speeds are 13.8 knots, 12.1 knots, and 11.1 knots at low, base case, and high fuel prices, respectively. When in-transit inventory costs are considered, laden speeds on both SCR and Cape routes become 16 knots, 14.1 knots, and 13 knots, at low, base case, and high fuel/commodity prices, respectively. Laden speeds on the NSR become 13.7 knots, 12.3 knots, and 11.6 knots, at low, base case, and high fuel/commodity prices, respectively. Similar relationships between optimal ballast and laden/laden with inventory speeds are expected for other fuel types and operational modes.

The SCR-NSR RFR and Cape-NSR RFR differentials range from 0.1 / -0.5 to 0.2 / 0.5 and -4.5 / -3.6 US$/t at low, base case, and high fuel price scenarios, whereas they become 0.5 / 0.5, 1.4 / 3.2, and -2.2 / 1.1 US$/t at each scenario respectively when in-transit inventory is considered. Similarly, the SCR-Cape RFR differential ranges from 0.6 (0) to -0.3 (-1.7) to -0.9 (-3.4) US$/t at low, base case and high fuel price scenarios without and with in-transit inventory costs, respectively. As a result, when in-transit inventory costs are included in the model,

shorter route alternatives are always benefitted, depending on commodity and fuel prices. Yet, the lower the fuel and commodity prices, the more competitive a longer route becomes and vice versa. Moreover, when the value of cargo is not considered in the analysis, this further increases the competitiveness of a longer route when moving towards low fuel and commodity prices. For example, the minimum Cape RFR is on par with the minimum SCR RFR, whilst the NSR is more competitive than Cape by 0.5 US$/t at the low fuel/commodity price scenario. However, if in-transit inventory costs are not included in the model, the Cape route becomes more competitive than SCR and NSR by 0.6 and 0.5 US$/t, respectively. Similar observations can be made between the SCR and NSR, where the RFR differential is reduced from 0.5 to 0.1 US$/t when in-transit inventory is not included at the low fuel/commodity price scenario. This effect can have certain implications for route choice and transport costs, also depending on the structure of the market (either contango or backwardation between the origin and destination ports), and therefore the value of transit time, and the difference between total landed costs and revenue when the cargo reaches its destination.

Low VLSFO/MGO & Jet Fuel/Gasoil Prices – High USD/RUB Rate

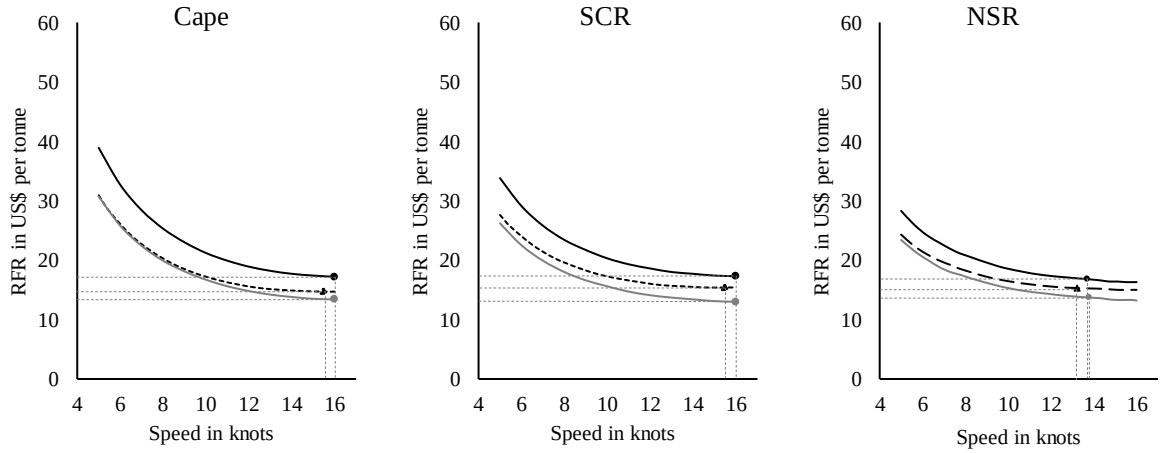


Base Case

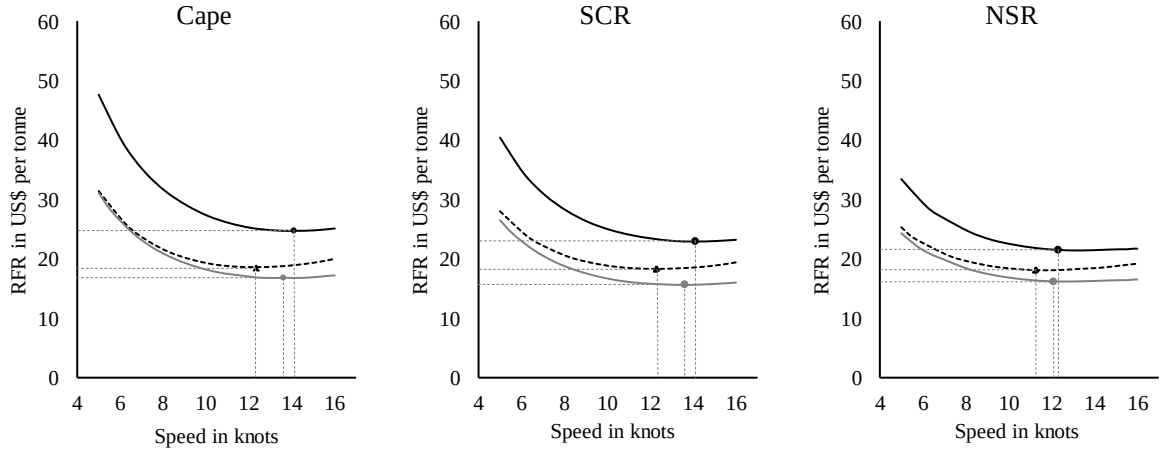


High VLSFO/MGO & Jet Fuel/Gasoil Prices – Low USD/RUB Rate

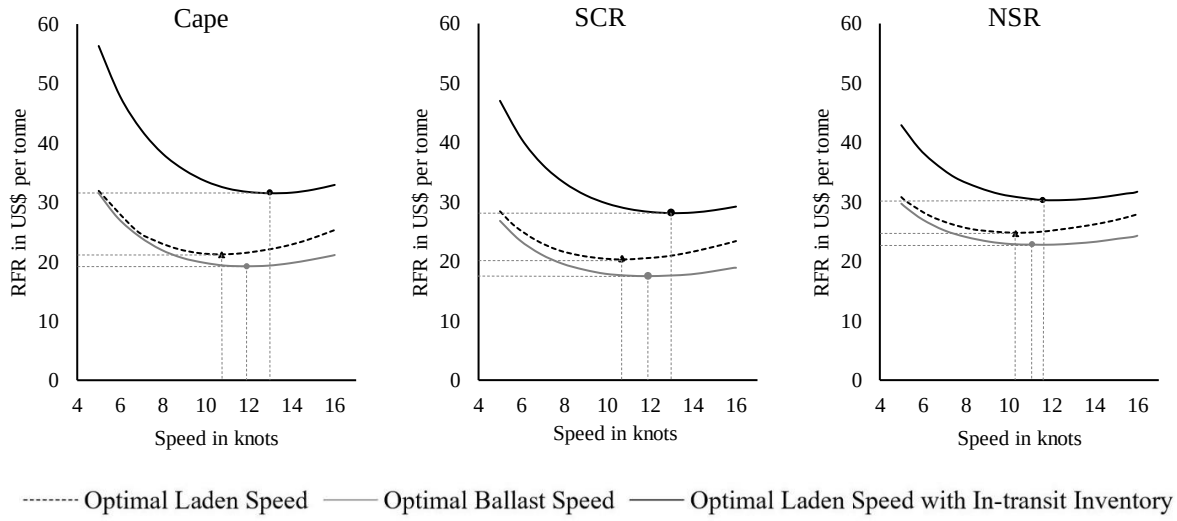


Figure 3. Relationship between LR2 tanker optimal laden and ballast speed, with and without in-transit inventory cost for Ulsan-Rotterdam OD pair at VLSFO mode, all route alternatives and scenarios.

### *4.2 Optimal ship speed and alternative operational modes*

Figure 4 depicts the relationship between optimal laden speed, including in-transit inventory costs, and minimum RFR across all routes and alternative operational modes using the Ulsan-Rotterdam OD pair at the base case fuel/commodity prices as an example. Similar to Figure 3, the minimum RFR is shown in the vertical axis as a function of optimal speed, which is shown in the horizontal axis. Black solid curves show the minimum RFR at the HSFO-Scrubber mode and black dashed curves show the minimum RFR at the VLSFO mode. Grey solid curves show the minimum RFR at the dual-fuel LNG-VLSFO option with a tank capacity of 1,700 $m^3$, whereas grey dotted curves illustrate the minimum RFR at the dual-fuel LNG-VLSFO option with a tank capacity of 3,600 $m^3$.

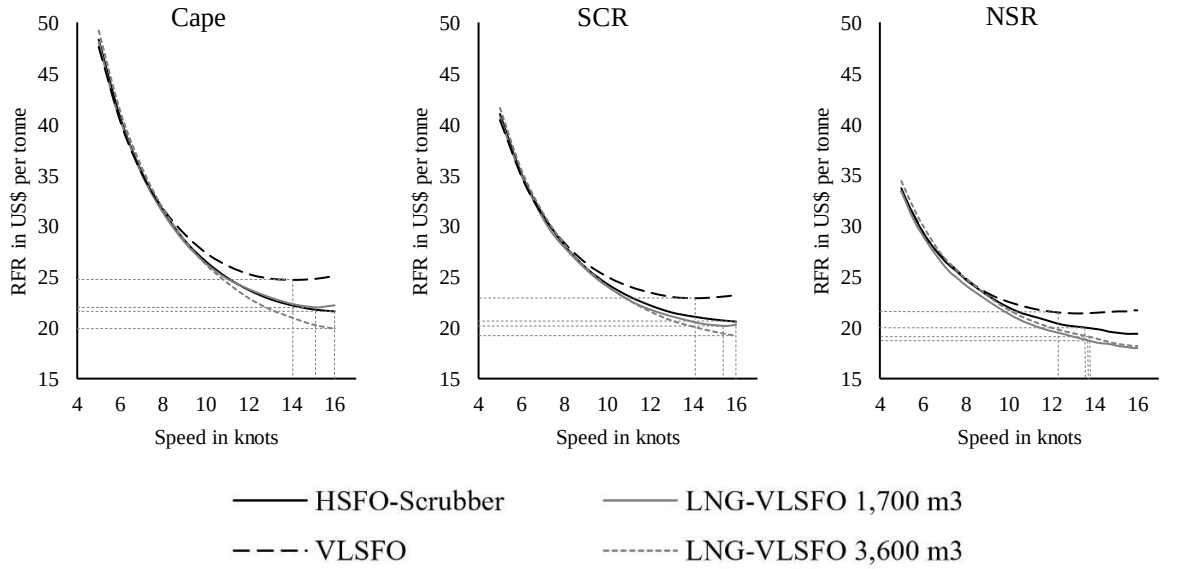


Figure 4. LR2 tanker minimum RFR at optimal speed for Ulsan-Rotterdam OD pair at all route alternatives and operational modes under Base Case Scenario.

Figure 4 shows that the lowest costs are found under the LNG-VLSFO mode for each route alternative. The lowest RFR for the SCR and Cape routes is found at the sub-mode of 3,600 $m^3$, whereas the lowest NSR RFR is found at the sub-mode of 1,700 $m^3$. This difference for the NSR can be explained by the fact that capital costs of the 3,600 $m^3$ sub-mode are higher than those of the 1,700 $m^3$ sub-mode. On one hand, the use of a tank capacity of 3,600 $m^3$ on the SCR and Cape routes allows the use of the low-priced LNG only, for the whole voyage compared to the other fuel alternatives, based on prices as of February 2020. Thus, lower voyage costs outweigh the increase in capital costs. On the other hand, the range under which the shorter NSR can be benefitted by the use of LNG is already high under the 1,700 $m^3$ sub-mode, and therefore the increase in capital costs is more pronounced on this route than on SCR and Cape[5]. The HSFO-Scrubber option comes third for the SCR and NSR. However, HSFO-Scrubber comes second for the Cape route, followed by the 1,700 $m^3$ sub-mode, since the minimum Cape RFR is disadvantaged by the large proportion of VLSFO at this LNG-VLSFO sub-mode. The VLSFO mode is the most expensive for each route alternative. Similar observations can be made for the rest OD pairs, where the ranking of each operational mode varies with respect to distance, fuel and commodity price levels, as well as optimal speed levels and/or real speed levels.

### *4.3 Optimal and real ship speeds, alternative operational modes, distance, and route choice*

Figures 5a – 5c illustrate RFR rates for the Cape, SCR and NSR routes across all OD pairs, operational modes, and fuel/commodity prices. Numerical results are reported in Appendix E1. All results refer to laden voyages, including in-transit inventory costs, and are based in two distinct speed regimes. The upper part of each of the Figures 5a – 5c shows results when speeds are optimised with respect to costs and market factors, whereas the lower part shows results at a constant speed of 12 knots, considering actual speed choice from historic voyages between the Far East and Europe in 2014-2020 (see 3.1.2. for the methodological approach). Results for the NSR include RFR rates at discounted fees under high fuel/commodity prices to reflect a flexible marketing practice that the Northern Sea Route Administration could adopt, similar to that during 2011-2013, where high USD/RUB exchange rates combined with very high fuel prices rendered NSR transits very expensive at official icebreaking fees.

First, it can be seen that Cape is always more competitive than SCR across all OD pairs at low fuel/commodity prices and optimal speeds under HSFO-Scrubber and LNG-VLSFO 3,600 $m^3$ modes. It is on par with SCR on the short and medium-hauls at low fuel/commodity prices and optimal speeds under VLSFO and marginally uncompetitive under LNG-VLSFO 1,700 $m^3$. The Cape route becomes less competitive than SCR across all OD pairs at the base case and high fuel/commodity price scenarios, and optimal speeds under all operational modes. The biggest losses are realised under the LNG-VLSFO 1,700 $m^3$ mode, whereas the least losses are realised under the LNG-VLSFO 3,600 $m^3$ mode. The Cape route becomes uncompetitive across all OD pairs at low fuel/commodity prices and a constant speed of 12 knots under all operational modes. Moreover, it becomes more uncompetitive across all OD pairs at the base case and high fuel/commodity price scenarios under the constant speed of 12 knots than under an optimal speed regime across all operational modes. The exception is the LNG-VLSFO 1,700 $m^3$ sub-mode, where the LNG/VLSFO distance ratio gets higher as the use of LNG fuel is

[5] The distance leg under which VLSFO is used on the NSR at the 1,700 $m^3$ sub-mode is 188 n.m., compared to 6,571 n.m. and 3,144 n.m. on the Cape and SCR routes, respectively.

increased with lower speed. As a result, the SCR-Cape RFR differential is reduced at the constant speed regime compared to the RFR differential under the optimal speed regime.

Second, the NSR is less competitive than Cape on the long-haul at low fuel/commodity prices across all operational modes, regardless of the speed regime, as well as on the medium-haul at low fuel/commodity prices and optimal speeds under HSFO-Scrubber and LNG-VLSFO 3,600 $m^3$ modes. It is also less competitive than Cape on the long-haul at the base case scenario and optimal speeds under HSFO-Scrubber and LNG-VLSFO 3,600 $m^3$ modes. The NSR is always more competitive than Cape on the short haul across all fuel/commodity prices, speed regimes and operational modes.

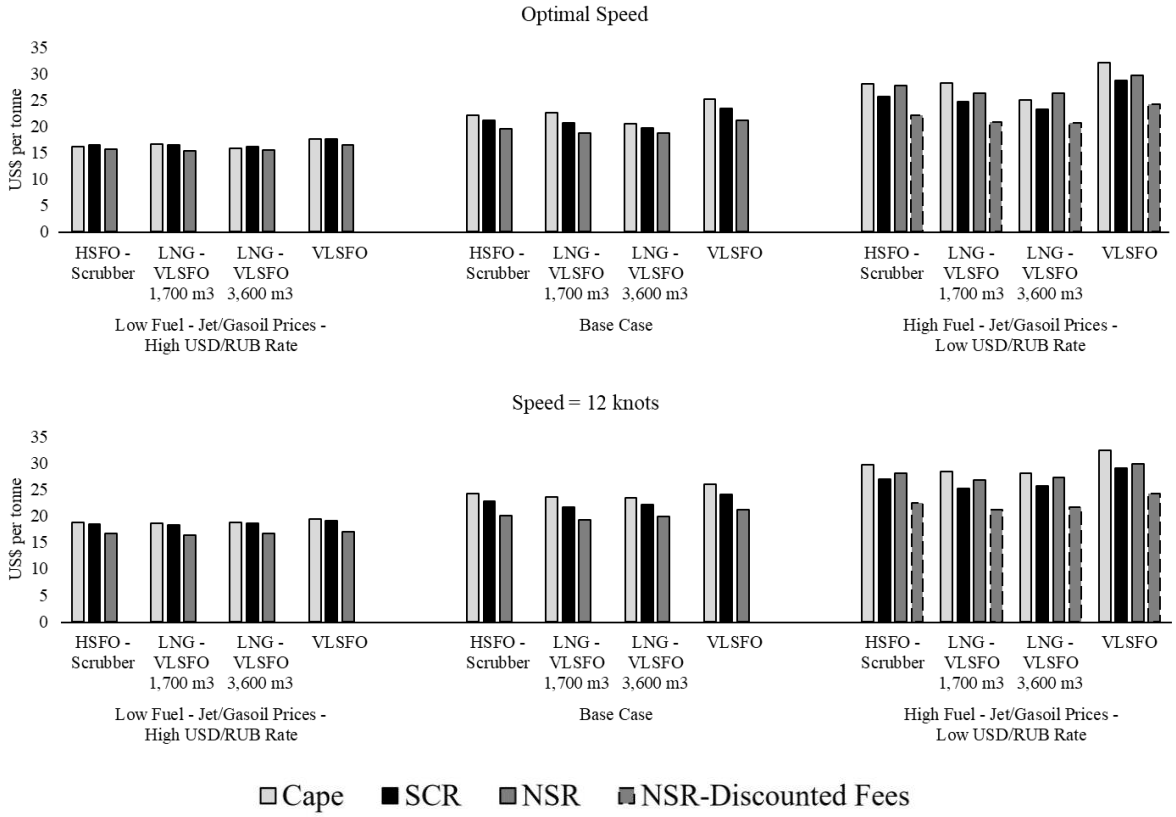


Figure 5a. RFR comparison at two speed regimes across all route alternatives, operational modes and scenarios for the Chiba – Coryton OD pair.

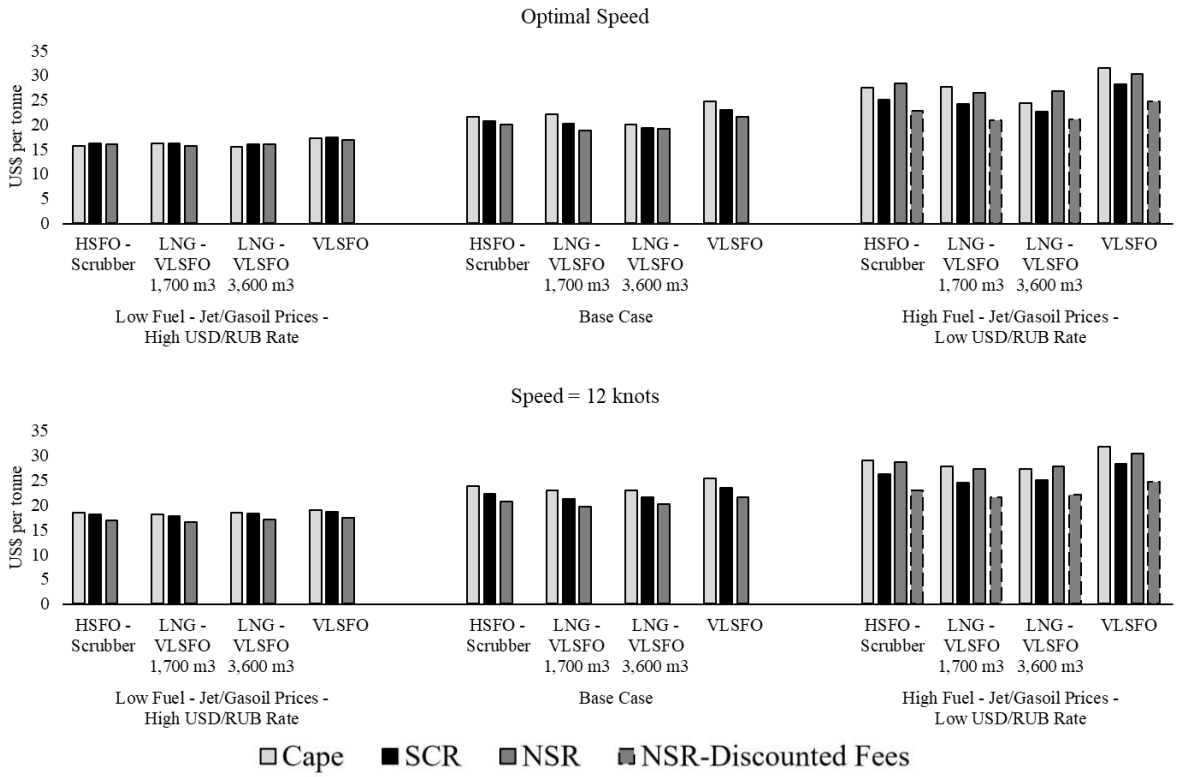


Figure 5b. RFR comparison at two speed regimes across all route alternatives, operational modes and scenarios for the Ulsan – Rotterdam OD pair.

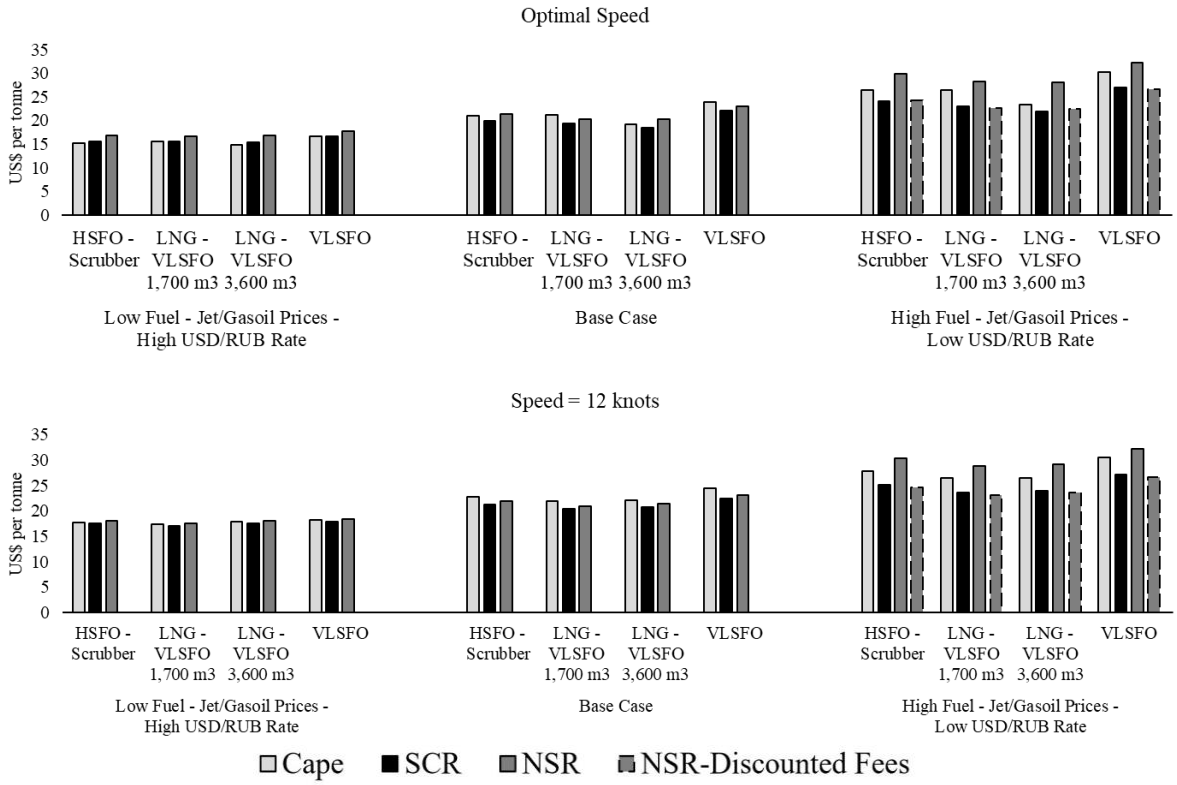


Figure 5c. RFR comparison at two speed regimes across all route alternatives, operational modes and scenarios for the Ulsan – Bilbao OD pair.

It is also more competitive than Cape on the medium-haul across all price scenarios and speed regimes under VLSFO and LNG-VLSFO 1,700 $m^3$ modes. Yet, the NSR is less competitive than Cape, especially on the long-haul, at high fuel/commodity prices, regardless of speed regime, and operational modes. It is also less competitive than Cape on the medium haul at high fuel/commodity prices and both speed regimes under HSFO-Scrubber and LNG-VLSFO 3,600 $m^3$ modes.

Third, the NSR is more competitive than SCR on the short and medium-hauls at low and base case fuel/commodity price scenarios and both speed regimes under all operational modes, whereas it is not competitive on the long-haul, regardless of fuel/commodity price levels, speed regime and operational mode. Yet, the NSR is less competitive than SCR across all OD pairs at high fuel/commodity prices and both speed regimes under all operational modes. On one hand, the competitiveness of the NSR is reduced at low fuel prices across all OD pairs, speed regimes and operational modes. On the other hand, high icebreaking fees owing to a low USD/RUB rate reduce the potential of the NSR at high fuel/commodity price levels. The NSR becomes more competitive than SCR and Cape across all OD pairs at high fuel/commodity prices and constant speeds under all operational modes, when assuming discounted fees. The NSR reduces its losses against the SCR on the long-haul at high fuel/commodity prices and optimal speeds under HSFO-Scrubber and LNG-VLSFO 3,600 $m^3$ modes when assuming discounted fees.

Table 5. Sensitivity Analysis for Ulsan-Rotterdam OD pair.

| ΔRFR | Low Fuel - Jet/Gasoil Prices – High USD/RUB rate | | | | Base Case | | | | | | High Fuel - Jet/Gasoil Prices – Low USD/RUB rate | | | | | |
|---|---|---|---|---|---|---|---|---|---|---|---|---|---|---|---|---|
| | Official Fees | Independent Navigation | Official Fees | Independent Navigation | Official Fees | Discounted Fees | Independent Navigation | Official Fees | Discounted Fees | Independent Navigation | Official Fees | Discounted Fees | Independent Navigation | Official Fees | Discounted Fees | Independent Navigation |
| | HSFO-Scrubber | | MGO in NSR | | HSFO-Scrubber | | | MGO in NSR | | | HSFO-Scrubber | | | MGO in NSR | | |
| | Optimal Speed | | | | | | | | | | | | | | | |
| SCR-NSR | 0.2 | 5.0 | 0.0 | 4.8 | 0.7 | 1.1 | 6.1 | 0.4 | 0.8 | 5.8 | -3.2 | 2.4 | 7.4 | -3.7 | 1.9 | 6.9 |
| | (-2.7) | (2.1) | (-2.9) | (1.9) | (-2.4) | (-1.9) | (3.1) | (-2.7) | (-2.2) | (2.8) | (-6.4) | (-0.8) | (4.2) | (-6.8) | (-1.2) | (3.8) |
| Cape-NSR | -0.2 | 4.6 | -0.4 | 4.4 | 1.7 | 2.2 | 7.2 | 1.4 | 1.8 | 6.8 | -0.8 | 4.8 | 9.8 | -1.3 | 4.4 | 9.4 |
| | (-3.1) | (1.7) | (-3.3) | (1.5) | (-1.4) | (-0.9) | (4.1) | (-1.7) | (-1.2) | (3.8) | (-4.0) | (1.6) | (6.6) | (-4.4) | (1.2) | (6.2) |
| SCR-Cape | 0.4 | | 0.4 | | -1.0 | | | -1.0 | | | -2.4 | | | -2.4 | | |
| | 12 knots | | | | | | | | | | | | | | | |
| SCR-NSR | 1.2 | 6.0 | 1.1 | 5.9 | 1.6 | 2.1 | 7.1 | 1.3 | 1.8 | 6.8 | -2.4 | 3.2 | 8.2 | -2.9 | 2.7 | 7.7 |
| | (-1.8) | (3.0) | (-2.0) | (2.8) | (-1.5) | (-1.0) | (4.0) | (-1.8) | (-1.3) | (3.7) | (-5.6) | (0.0) | (5.0) | (-6.1) | (-0.5) | (4.5) |
| Cape-NSR | 1.4 | 6.2 | 1.3 | 6.1 | 3.1 | 3.6 | 8.6 | 2.8 | 3.3 | 8.3 | 0.3 | 5.9 | 10.9 | -0.1 | 5.5 | 10.5 |
| | (-1.6) | (3.2) | (-1.7) | (3.1) | (0.0) | (0.5) | (5.5) | (-0.3) | (0.2) | (5.2) | (-2.9) | (2.8) | (7.8) | (-3.3) | (2.3) | (7.3) |
| SCR-Cape | -0.2 | | -0.2 | | -1.5 | | | -1.5 | | | -2.8 | | | -2.8 | | |
| | VLSFO | | MGO in NSR | | VLSFO | | | MGO in NSR | | | VLSFO | | | MGO in NSR | | |
| | Optimal Speed | | | | | | | | | | | | | | | |
| SCR-NSR | 0.5 | 5.3 | 0.5 | 5.3 | 1.4 | 1.9 | 6.9 | 1.4 | 1.9 | 6.9 | -2.2 | 3.4 | 8.4 | -2.2 | 3.4 | 8.4 |
| | (-2.5) | (2.3) | (-2.5) | (2.3) | (-1.7) | (-1.2) | (3.8) | (-1.7) | (-1.2) | (3.8) | (-5.5) | (0.1) | (5.1) | (-5.5) | (0.1) | (5.1) |
| Cape-NSR | 0.5 | 5.3 | 0.5 | 5.3 | 3.2 | 3.7 | 8.7 | 3.2 | 3.7 | 8.7 | 1.1 | 6.7 | 11.7 | 1.1 | 6.7 | 11.7 |
| | (-2.5) | (2.3) | (-2.5) | (2.3) | (0.0) | (0.5) | (5.5) | (0.0) | (0.5) | (5.5) | (-2.2) | (3.4) | (8.4) | (-2.2) | (3.4) | (8.4) |
| SCR-Cape | 0.0 | | 0.0 | | -1.7 | | | -1.7 | | | -3.4 | | | -3.4 | | |
| | 12 knots | | | | | | | | | | | | | | | |
| SCR-NSR | 1.3 | 6.1 | 1.3 | 6.1 | 1.8 | 2.3 | 7.3 | 1.8 | 2.3 | 7.3 | -2.1 | 3.5 | 8.5 | -2.1 | 3.5 | 8.5 |
| | (-1.8) | (3.0) | (-1.8) | (3.0) | (-1.4) | (-0.9) | (4.1) | (-1.4) | (-0.9) | (4.1) | (-5.4) | (0.2) | (5.2) | (-5.4) | (0.2) | (5.2) |
| Cape-NSR | 1.6 | 6.4 | 1.6 | 6.4 | 3.7 | 4.2 | 9.2 | 3.7 | 4.2 | 9.2 | 1.3 | 7.0 | 12.0 | 1.3 | 6.9 | 11.9 |
| | (-1.4) | (3.4) | (-1.4) | (3.4) | (0.5) | (1.0) | (6.0) | (0.5) | (1.0) | (6.0) | (-2.0) | (3.6) | (8.6) | (-2.0) | (3.6) | (8.6) |
| SCR-Cape | -0.4 | | -0.4 | | -1.9 | | | -1.9 | | | -3.4 | | | -3.4 | | |
| | LNG-VLSFO at 1,700 $m^3$ | | LNG-VLSFO at 3,600 $m^3$ | | LNG-VLSFO at 1,700 $m^3$ | | | LNG-VLSFO at 3,600 $m^3$ | | | LNG-VLSFO at 1,700 $m^3$ | | | LNG-VLSFO at 3,600 $m^3$ | | |
| | Optimal Speed | | | | | | | | | | | | | | | |
| SCR-NSR | 0.6 | 5.4 | 0.0 | 4.8 | 1.4 | 1.9 | 6.9 | 0.2 | 0.7 | 5.7 | -2.4 | 3.2 | 8.2 | -4.1 | 1.5 | 6.5 |
| | (-2.3) | (2.5) | (-2.9) | (1.9) | (-1.6) | (-1.1) | (3.9) | (-2.8) | (-2.3) | (2.7) | (-5.4) | (0.2) | (5.2) | (-7.1) | (-1.5) | (3.5) |
| Cape-NSR | 0.6 | 5.4 | -0.4 | 4.4 | 3.2 | 3.7 | 8.7 | 0.8 | 1.3 | 6.3 | 1.1 | 6.7 | 11.7 | -2.4 | 3.2 | 8.2 |
| | (-2.2) | (2.6) | (-3.3) | (1.5) | (0.3) | (0.8) | (5.8) | (-2.1) | (-1.7) | (3.3) | (-1.9) | (3.7) | (8.7) | (-5.4) | (0.2) | (5.2) |
| SCR-Cape | -0.1 | | 0.4 | | -1.8 | | | -0.6 | | | -3.5 | | | -1.7 | | |
| | 12 knots | | | | | | | | | | | | | | | |
| SCR-NSR | 1.1 | 5.9 | 1.1 | 5.9 | 1.4 | 1.9 | 6.9 | 1.4 | 1.9 | 6.9 | -2.7 | 2.9 | 7.9 | -2.7 | 2.9 | 7.9 |
| | (-1.9) | (2.9) | (-1.9) | (2.9) | (-1.6) | (-1.1) | (3.9) | (-1.6) | (-1.1) | (3.9) | (-5.8) | (-0.2) | (4.8) | (-5.8) | (-0.2) | (4.8) |
| Cape-NSR | 1.5 | 6.3 | 1.4 | 6.2 | 3.2 | 3.7 | 8.7 | 2.7 | 3.2 | 8.2 | 0.4 | 6.0 | 11.0 | -0.4 | 5.3 | 10.3 |
| | (-1.5) | (3.3) | (-1.6) | (3.2) | (0.1) | (0.6) | (5.6) | (-0.3) | (0.2) | (5.2) | (-2.7) | (3.0) | (8.0) | (-3.4) | (2.2) | (7.2) |
| SCR-Cape | -0.4 | | -0.2 | | -1.8 | | | -1.3 | | | -3.2 | | | -2.4 | | |

Note: RFR Differentials in parentheses refer to results when ice damage repairs are factored in the analysis.

### *4.4 Sensitivity Analysis*

The results are tested against different fuel/commodity price and icebreaking fees levels, the assumption of ice damage repairs, and a future prohibition on the use of heavy fuel oils in the Arctic (either HSFO, including with the use of scrubbers, or VLSFO). Table 5 presents sensitivity analysis results across all routes, fuel/commodity price levels, and speed regimes, using the Ulsan-Rotterdam pair as an example. Results for the rest OD pairs are presented in Appendix E1. It can be seen that the use of MGO through ice on NSR by oil-powered tankers reduces the competitiveness of NSR compared to both Cape and SCR under HSFO-Scrubber, especially when moving towards higher fuel/commodity prices. The impact is similar either at optimal or constant speed regimes and both with and without icebreaking fees. This is the result of a wide HSFO-MGO price differential between 100 (low prices) and 300 US$/t (high prices). The difference is negligible on the VLSFO mode, where the VLSFO-MGO price differential ranges between 10 (low prices) and 30 US$ (high prices). The NSR becomes uncompetitive across all scenarios and under all operational modes when including ice damage repairs in the analysis. It is only more competitive than Cape on the short and medium-hauls at the base case scenario under HSFO and constant speeds, under VLSFO at both speed regimes, including with the use of MGO through ice on NSR, as well as under LNG-VLSFO 1,700 $m^3$ at both speed regimes. The competitiveness of the NSR increases under discounted fees across all scenarios, whilst the route is more competitive than both SCR and Cape under independent navigation, regardless of fuel/commodity price levels.

The highest SCR-NSR and Cape-NSR RFR differentials are found at the high fuel/commodity price scenario under the assumption of independent navigation. The highest SCR-NSR and Cape-NSR RFR differentials at optimal speeds are found under VLSFO, followed by LNG-VLSFO 1,700 $m^3$, HSFO, and LNG-VLSFO 3,600 $m^3$ modes respectively. The highest SCR-NSR RFR differential at constant speed is found under VLSFO, followed by HSFO, LNG-VLSFO 1,700 $m^3$ and 3,600 $m^3$ modes, respectively. The highest Cape-NSR differentials are the same as those at the optimal speed regime. When including ice damage repairs, the LNG-VLSFO 1,700 $m^3$ mode comes first, followed by VLSFO, HSFO, and LNG-VLSFO 3,600 $m^3$ modes for both SCR-NSR and Cape-NSR RFR differentials at optimal speeds, respectively. Yet, the order of modes for RFR differentials at constant speeds is the same as that when ice damage repairs are not considered. Similar results are obtained for the other OD pairs, with differences being attributed to different OD distances.

## 5. Discussion and conclusions

This paper contributes to Arctic shipping literature in several ways. It contributes to knowledge by assessing the economic potential of the NSR for tankers carrying oil products between the Far East and Europe, based on historic NSR transits and typical arbitrage trade flows. It contributes to theory by considering in-transit inventory costs along with fuel prices to link market structure and route choice in the context of oil product tanker flows between east and west. Not only is the NSR compared with SCR, but also the Cape route is included to explain route choice for oil product tanker trades between Northeast Asia and Europe, based on cost factors and market developments which favour longer or shorter routes. The cost-based analysis explains route choice depending on two distinct states of the market. First, it explains the choice of shorter routes when cargo value is important and fuel and commodity prices are high. Second, it explains the choice of longer routes when cargo value is not critical and fuel and commodity prices are low. It contributes to methodology by developing an approach which

has two objectives. First, the cost assessment is based on speed optimisation, which minimises the RFR of a route. Second, the cost assessment is based on real speeds, drawing from AIS data of LR2 tanker voyages between Northeast Asia and Europe. It contributes to practice and policy in two main ways. First, route choice is explained depending on varying cost factors and market conditions. Second, alternative operational modes are considered to assess how current and future emissions regulations at both the local and global levels affect route choice (IMO sulphur limit, Initial IMO GHG strategy, future prohibition on the use of heavy fuel oils in the Arctic). The alternative operational modes refer to oil and gas-based fuels (HSFO, VLSFO, MGO, LNG), as well as current and future technologies with respect to LNG fuel tank capacity, i.e. 1,700 $m^3$ and 3,600 $m^3$, respectively.

The NSR is more competitive under high fuel/commodity prices, independent navigation, and high-priced fuel options/modes (VLSFO, LNG-VLSFO 1,700 $m^3$) across all OD pairs and optimal speeds. Longer routes (SCR, Cape) increase their competitiveness when moving towards longer OD pairs and vice versa, depending on operational mode, prices, and speed regime. Shorter routes are favoured when in-transit inventory is considered, since the value of cargo becomes the most important factor when moving from lower to higher commodity prices, and from longer to shorter hauls. Shorter routes are favoured at the constant speed of 12 knots since transit times for longer routes increase more than those for shorter routes and result in comparatively higher fuel and fixed costs. The competitiveness of a longer route over a shorter route increases under low-priced fuel options/modes (HSFO, LNG-VLSFO 3,600 $m^3$), lower fuel/commodity prices, higher LNG/VLSFO distance ratios (such as under LNG-VLSFO 3,600 $m^3$, see Appendix D1) and vice versa. Longer routes increase their competitiveness/reduce their losses under LNG-VLSFO 1,700 $m^3$ at the constant speed of 12 knots rather than at optimal speeds since LNG mileage increases with lower speeds and therefore the LNG/VLSFO distance ratio gets higher (see Appendix D1). Laden speeds are higher than ballast speeds when in-transit inventory is considered, with lower differentials on NSR owing to speed constraints on ice. A prohibition on the use of heavy fuel oils in the Arctic (HSFO, VLSFO) reduces the competitiveness of the NSR, either at optimal or constant speed regimes, depending on the HSFO-MGO and VLSFO-MGO price differentials. Ice damage repairs render the NSR uncompetitive across all OD pairs and operational modes under official icebreaking fees, with the route being competitive only against Cape at the base case and VLSFO (including with the use of MGO through ice on NSR) and LNG-VLSFO 1,700 $m^3$ modes on the short and medium hauls.

This study complements that of Theocharis et al. (2019), by incorporating in-transit inventory costs in the analysis, dual-fuel Oil/LNG modes, and addressing market structure and route choice in the context of oil product tanker flows between east and west. Not only is the NSR compared with SCR, but also the Cape route is included to explain why longer routes and delays of arrivals are favoured when market conditions are similar to those during the collapse of oil prices and the subsequent oil oversupply during 2015-2017 and that during 2020. The results show that Cape is more competitive than both the SCR and NSR when moving from short to long hauls and under low fuel/commodity prices. Although Cape is marginally uncompetitive under real speeds, it may still be chosen, depending on OD distances, operational modes and fuel prices if the contango is wide enough to more than compensate a charterer at the time of delivery. Yet, regional supply and demand factors determine actual freight rate levels, which may or may not be higher than those for other routes, such as the SCR. This point emphasises that freight is part of the total landed price of the cargo, and route choice is not considered solely on absolute transport cost differences. Freight is important when commodity prices are high and futures prices are lower than spot prices, and therefore quick

deliveries and shorter routes are favoured. Although oil oversupply is generally linked with low prices and contango structure, backwardation may not always concur with high spot commodity prices. For example, persistent contango in ICE gasoil futures prices during 2011 and for some part of 2013 occurred at historically high oil products and fuel price levels. Figure A1 illustrates that point, where some Cape voyages occurred even during 2013, as well as in 2018, a year where prices had increased following a steep drop during 2015-2017. The results also show that route competitiveness depends on operational mode and technology as much as it depends on fuel price levels. Whilst a low-priced LNG favours the shorter NSR at LNG-VLSFO 1,700 $m^3$, depending on OD distances, a larger LNG tank capacity reduces this benefit. Yet, market factors and the adoption of more than one fuel type/technology could increase the versatility of a tanker.

Future research could examine other commodities, trade flows, the Suez Canal toll policies regarding rebates at times of low transport costs, as well as various fuel price differentials, especially that of HSFO-VLSFO in light of the recent spread volatility, and the relationship between LNG and oil-based fuel prices in various hubs. Finally, speed-dependent fuel consumption elasticities could be employed to address the fact that the cubic law between speed and fuel consumption does not hold at speeds lower than the design speed of a tanker (Adland, Cariou, and Wolff, 2020), which can have implications for certain routes and distances, as well as for fuel consumption through ice on the NSR.

## Notes

1. Another two LR2 laden voyages were conducted in 2013, but these involved naphtha cargoes from Europe to the Far East (CHNL 2021).

2. This is known as ‘backwardation’ and occurs when the price of a commodity trading in the futures market is lower than the spot price.

3. This is known as ‘contango’ and occurs when the future price of a commodity is higher than the spot price i.e. the opposite of backwardation.

4. An OD pair linking Northeast Asian ports with the UK is chosen instead of France due to proximity of the later with the biggest importer i.e., the Netherlands.

5. The distance leg under which VLSFO is used on the NSR at the 1,700 m3 sub-mode is 188 n.m., compared to 6,571 n.m. and 3,144 n.m. on the Cape and SCR routes, respectively.

## Acknowledgements

This work was supported by the Economic and Social Research Council [ESRC] Wales Doctoral Training Partnership Studentship No. T90363D. The authors are grateful to three anonymous marine engineers at MAN Energy Solutions (https://marine.man-es.com/two-stroke/ceas) who provided detailed information and help with dual-fuel engine set-ups, and two-stroke engines power-consumption calculations.

## Disclosure statement

No potential conflict of interest was reported by the authors.

## References


Adland, R., P. Cariou, and F-C. Wolff. 2020. “Optimal ship speed and the cubic law revisited: Empirical evidence from an oil tanker fleet.” *Transportation Research Part E: Logistics and Transportation Review* 140: 101972. doi: 10.1016/j.tre.2020.101972.

Bloomberg. 2021. Bloomberg Terminal.

Clarksons. 2021. *Clarksons Shipping Intelligence Network*, https://sin.clarksons.net

CHNL. 2021. “Statistics.” *CHNL*, https://arctic-lio.com/

Dataloy. 2020. *Dataloy Distance Table*, https://ddt.dataloy.com

Ding, W., Y. Wang, L. Dai, and H. Hu. 2020. “Does a carbon tax affect the feasibility of Arctic shipping?” *Transportation Research Part D: Transport and Environment* 80: 102257. doi: 10.1016/j.trd.2020.102257.

DNV. 2021. Veracity Platform. *DNV*, https://www.veracity.com/

Faury, O., and P. Cariou. 2016. “The Northern Sea Route competitiveness for oil tankers.” *Transportation Research Part A: Policy and Practice* 94: 461–469. doi: 10.1016/j.tra.2016.09.026.

Faury, O., A. Cheaitou, and P. Givry. 2020. “Best maritime transportation option for the Arctic crude oil: A profit decision model.” *Transportation Research Part E: Transportation and Logistics* Review 136: 1–21. doi: 10.1016/j.tre.2020.101865.

IEA. 2020. International Energy Agency: Oil Information (2020 Edition). UK Data Service, https://doi.org/10.5257/iea/oil/2020

Keltto, T., and S-H. Woo. 2019. “Profitability of the Northern Sea Route for liquid bulk shipping under post 2020 sulphur regulations.” *International Journal of Logistics Management* 31 (2): 313–332. doi: 10.1108/IJLM-12-2018-0314.

Lasserre, F. 2014. “Case studies of shipping along Arctic routes. analysis and profitability perspectives for the container sector.” *Transportation Research Part A: Policy and Practice* 66: 144–161. doi: 10.1016/j.tra.2014.05.005.

MAN Energy Solutions. 2019. “CEAS Engine Calculations.” https://www.man-es.com/marine/products/planning-tools-and-downloads/ceas-engine-calculations

Meng, Q., Y. Zhang, and M. Xu. 2016. “Viability of transarctic shipping routes: a literature review from the navigational and commercial perspectives.” *Maritime Policy & Management* 44 (1): 1-26. doi: 10.1080/03088839.2016.1231428.

OPEC. 2021. “OPEC Monthly Oil Market Report.” *OPEC*, https://www.opec.org/opec_web/en/publications/338.htm

Psaraftis, H.N., and C. A. Kontovas. 2013. “Speed models for energy-efficient maritime transportation: A taxonomy and survey.” *Transportation Research Part C: Emerging Technologies* 26, 331–351. doi: 10.1016/j.trc.2012.09.012.

Refinitiv Eikon. 2021. Refinitiv Eikon Platform.

Shibasaki, R., T. Usami, M. Furuichi, H. Teranishi, and H. Kato. 2018. “How do the new shipping routes affect Asian liquefied natural gas markets and economy? Case of the Northern Sea Route and Panama Canal expansion.” *Maritime Policy & Management* 45 (4): 543–566. doi: 10.1080/03088839.2018.1445309.

Solakivi, T., T. Kiiski, and L. Ojala. 2018. “The impact of ice class on the economics of wet and dry bulk shipping in the Arctic waters.” *Maritime Policy & Management* 45 (4): 530–542. doi: 10.1080/03088839.2018.1443226.

Smith, L. C., and S. R. Stephenson. 2013. “New Trans-Arctic shipping routes navigable by midcentury.” *Proceedings of the National Academy of Science of the USA* 110 (13): 4871–4872. doi: 10.1073/pnas.1214212110.

Theocharis, D., S. Pettit, V. S. Rodrigues, and J. Haider. 2018. “Arctic shipping: a systematic literature review of comparative studies.” *Journal of Transport Geography* 69: 112 – 128. doi: 10.1016/j.jtrangeo.2018.04.010.

Theocharis, D., V. S. Rodrigues, S. Pettit, and J. Haider. 2019. “Feasibility of the Northern Sea Route: The role of distance, fuel prices, ice breaking fees and ship size for the product tanker market.” *Transportation Research Part E: Logistics and Transportation Review* 129, 111–135. doi: 10.1016/j.tre.2019.07.003.

Theocharis, D., V. S. Rodrigues, S. Pettit, J. Haider. 2021. “Feasibility of the Northern Sea Route for seasonal transit navigation: The role of ship speed on ice and alternative fuel types for the oil product tanker market.” *Transportation Research Part A: Policy and Practice* In press. doi: 10.1016/j.tra.2021.03.013.

Wang, D., R. Ding, Y. Gong, R. Wang, J. Wang, and X. Huang. 2020. “Feasibility of the Northern Sea Route for oil shipping from the economic and environmental perspective and its influence on China's oil imports.” *Marine Policy* 118: 104006. doi: 10.1016/j.marpol.2020.104006.

Wang, N., B. Tan, N. Wu, and W-J. Zhao. 2016. “Comments on “Case studies of shipping along Arctic routes. Analysis and profitability perspectives for the container sector””. *Transportation Research Part A: Policy and Practice* 94: 699–702. doi: 10.1016/j.tra.2016.09.004.

Wergeland, T. 1992. “The northern sea route - rosy prospects for commercial shipping?” *International Challenges* 12 (1): 43-57.

Xu, H., D. Yang, and J. Weng. 2018. “Economic feasibility of an NSR/SCR-combined container service on the Asia-Europe lane: a new approach dynamically considering sea ice extent.” *Maritime Policy & Management* 45 (4): 514–529. doi: 10.1080/03088839.2018.1443521.

Xu, H., and D. Yang. 2020. “LNG-fuelled container ship sailing on the Arctic Sea: Economic and emission assessment.” *Transportation Research Part D: Transport and Environment* 87, 102556. doi: 10.1016/j.trd.2020.102556.

Zhang, Y., Q. Meng, and S. H. Ng. 2016. “Shipping efficiency comparison between northern sea route and the conventional Asia-Europe shipping route via Suez Canal.” *Journal of Transport Geography* 57: 241–249. doi: 10.1016/j.jtrangeo.2016.09.008.

Zhao, H., Hua, H., Lin, Y., 2016. Study on China-EU container shipping network in the context of Northern Sea Route. *Journal of Transport Geography* 53: 50–60. doi: 10.1016/j.jtrangeo.2016.01.013

**Appendix A1.**

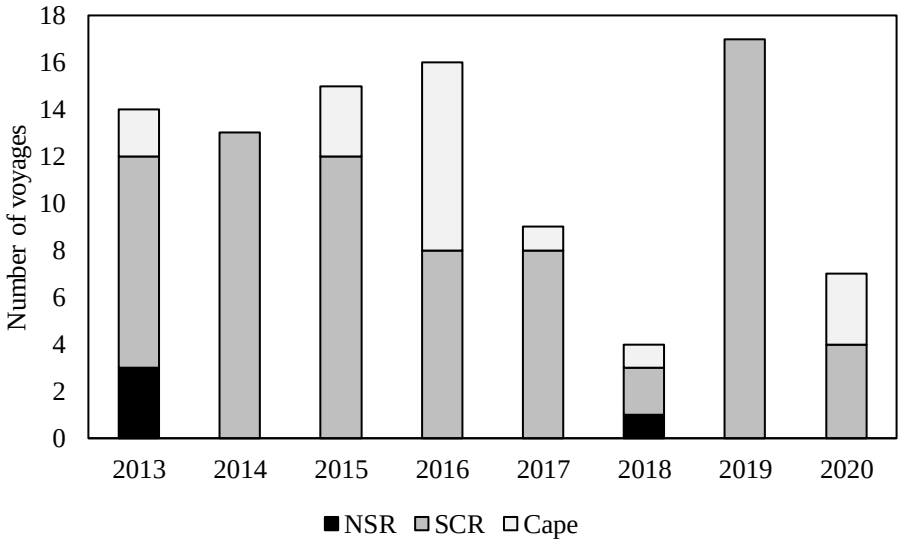


Sources: Refinitiv Eikon (2021), Bloomberg (2021).

Figure A1. Number of voyages conducted between Northeast Asia and Northwest Europe per route alternative between 2013 and 2020.

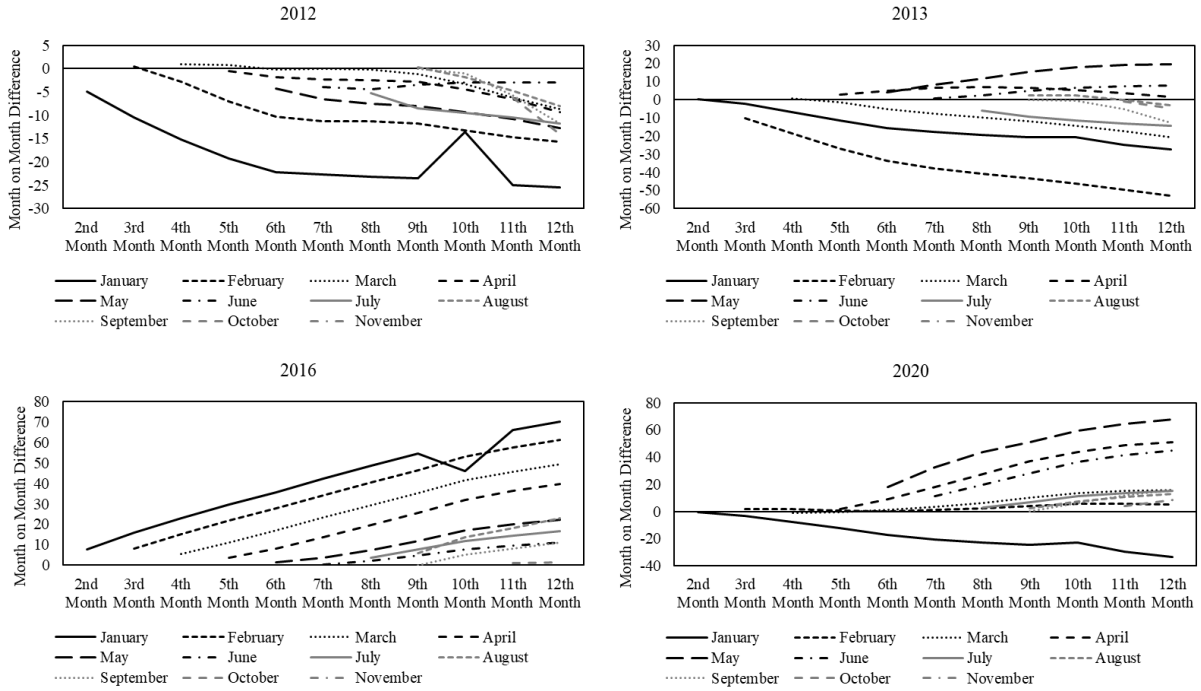


Source: Based on data from Bloomberg (2021). Notes: The figure shows futures curves of the Intercontinental Exchange (ICE) Gasoil Futures Contract, which is traded on the Intercontinental Exchange, and used as a price reference for distillates (jet fuel/kerosene, gasoil/diesel) in Europe by hedgers, arbitrageurs and speculators alike. Starting from January, the curves show for every year the future price of the contract in each successive month (1st day) ahead until December.

Figure A2. Historic ICE Low Sulphur Gasoil Futures Curves.


Sources: OPEC (2021), Clarksons (2021).

Figure A3. Jet fuel/kerosene and gasoil/diesel prices between 2011 and 2020.

**Appendix B1.** First and Second Order Conditions for the optimal speeds.

When a tanker operates on either HSFO-Scrubber or VLSFO mode (Equation (6)):

$$RFR = \frac{1}{W} \cdot \left[ \left( \frac{D_{SCR,NSR,Cape}}{S^*_{FO\,L,B} \cdot 24} \right) \cdot \left( \left( F_{FO}\left(S^*_{FO\,L,B}\right) \cdot P_{FO} \right) + (C_o + C_c + g \cdot C_s) + q \cdot (W \cdot P_C \cdot \frac{r}{365}) \right) + C_{TI} \right]$$

Assuming a fuel consumption function (Equation (1)):

$$F_{FO}(s^*, \nabla) = F_{FO\,d} \cdot \left( \frac{S^*_{FO\,L,B}}{S_d} \right)^a \cdot \left( \frac{P + L}{\nabla} \right)^{2/3}$$

The only decision variable is the speed, $s^*_{FO\,L,B}$, with the rest being data inputs to the problem.

By substituting Equation (1) into Equation (6):

$$RFR = \frac{1}{W} \cdot \left[ \left( \frac{D_{SCR,NSR,Cape}}{S^*_{FO\,L,B} \cdot 24} \right) \cdot \left( \left( F_{FO\,d} \cdot \left( \frac{S^*_{FO\,L,B}}{S_d} \right)^a \cdot \left( \frac{P + L}{\nabla} \right)^{2/3} \cdot P_{FO} \right) + (C_o + C_c + g \cdot C_s) + q \cdot (W \cdot P_C \cdot \frac{r}{365}) \right) + C_{TI} \right]$$

And by expanding:

$$RFR = \frac{D_{SCR,NSR,Cape} \cdot F_{FO\,d} \cdot {S^*_{FO\,L,B}}^{(a-1)} \cdot P_{FO} \cdot (P + L)^{\frac{2}{3}}}{W \cdot 24 \cdot {S_d}^a \cdot \nabla^{\frac{2}{3}}} + \frac{\left( (C_o + C_c + g \cdot C_s) + q \cdot \left( W \cdot P_C \cdot \frac{r}{365} \right) \right) \cdot D_{SCR,NSR,Cape}}{24 \cdot W} \cdot \frac{1}{S^*_{FO\,L,B}} + \frac{C_{TI}}{W}$$

The first order condition to obtain the optimal speed, $S^*_{FO\,L,B}$, which minimises the $RFR$ is $\frac{\partial RFR}{\partial S^*_{FO\,L,B}} = 0$:

$$\frac{(a-1)\cdot D_{SCR,NSR,Cape}\cdot F_{FO\,d}\cdot P_{FO}\cdot (P+L)^{\frac{2}{3}}}{W\cdot 24\cdot {S_d}^{a}\cdot \nabla^{\frac{2}{3}}}\cdot {S^*_{FO\,L,B}}^{(a-2)}-\frac{\left((C_o+C_c+g\cdot C_s)+q\cdot\left(W\cdot P_C\cdot\frac{r}{365}\right)\right)\cdot D_{SCR,NSR,Cape}}{W\cdot 24}\cdot\frac{1}{{S^*_{FO\,L,B}}^{2}}=0$$

And by rearranging, the optimal speed, $S^*_{FO\,L,B}$ is:

$${S^*_{FO\,L,B}}^{a}=\frac{\left((C_o+C_c+g\cdot C_s)+q\cdot\left(W\cdot P_C\cdot\frac{r}{365}\right)\right)\cdot {S_d}^{a}\cdot\nabla^{\frac{2}{3}}}{(a-1)\cdot F_{FO\,d}\cdot P_{FO}\cdot(P+L)^{\frac{2}{3}}}\quad\text{or}\qquad S^*_{FO\,L,B}=\sqrt[a]{\frac{\left((C_o+C_c+g\cdot C_s)+q\cdot\left(W\cdot P_C\cdot\frac{r}{365}\right)\right)\cdot {S_d}^{a}\cdot\nabla^{\frac{2}{3}}}{(a-1)\cdot F_{FO\,d}\cdot P_{FO}\cdot(P+L)^{\frac{2}{3}}}}$$

The second order condition is:

$$\frac{\partial^2 RFR}{\partial {S^*_{FO\,L,B}}^{2}}=\frac{(a-1)\cdot(a-2)\cdot D_{SCR,NSR,Cape}\cdot F_{FO\,d}\cdot P_{FO}\cdot(P+L)^{\frac{2}{3}}}{W\cdot 24\cdot {S_d}^{a}\cdot\nabla^{\frac{2}{3}}}\cdot {S^*_{FO\,L,B}}^{(a-3)}+\frac{2\cdot\left((C_o+C_c+g\cdot C_s)+q\cdot\left(W\cdot P_C\cdot\frac{r}{365}\right)\right)\cdot D_{SCR,NSR,Cape}}{W\cdot 24}\cdot\frac{1}{{S^*_{FO\,L,B}}^{3}}$$

For $a=3$ (cubic fuel consumption function):

$$=\frac{2\cdot D_{SCR,NSR,Cape}\cdot F_{FO\,d}\cdot P_{FO}\cdot(P+L)^{\frac{2}{3}}}{W\cdot 24\cdot {S_d}^{3}\cdot\nabla^{\frac{2}{3}}}+\frac{2\cdot\left((C_o+C_c+g\cdot C_s)+q\cdot\left(W\cdot P_C\cdot\frac{r}{365}\right)\right)\cdot D_{SCR,NSR,Cape}}{W\cdot 24}\cdot\frac{1}{{S^*_{FO\,L,B}}^{3}}$$

Substituting the data inputs and the value of the optimal speed obtained from the first order condition every time, it is proved that $\frac{\partial^2 RFR}{\partial {S^*_{FO\,L,B}}^{2}}>0$.

Thus the solution is unique and is a global minimum in $\underline{S}\le s^*\le\overline{S}$.

Similarly, the process of calculating the optimal speed when a tanker operates on dual-fuel Oil/LNG mode under VLSFO (Equation (7), is the same, where the binary variable, $b$, is set equal to zero, and the binary variable, $c$, is set equal to 1 in both cases. Moreover, optimal speeds when a tanker conducts ballast voyages for oil-based modes (Equation (8), is the same as above with the term $q\cdot\left(W\cdot P_C\cdot\frac{r}{365}\right)$, set equal to zero through the binary variable, $q$, and the binary variable, $g$, equals 1 under HSFO-Scrubber mode or zero under VLSFO mode. The only difference is the notation of speed and fuel consumption.

When a tanker operates on dual-fuel Oil/LNG mode and uses LNG as a fuel (Equation (7)):

$$RFR = \frac{1}{W} \cdot \left[ \left( \frac{D_{SCR,NSR,Cape}}{(S^*_{DF\ LNG\ L,B} + S^*_{DF\ FO\ L,B}) \cdot 24} \right) \cdot \left( b \cdot \left( F_{DF\ LNG}\left(S^*_{DF\ LNG\ L,B}\right) \cdot P_{LNG} + F_{DF\ Pilot}\left(S^*_{DF\ LNG\ L,B}\right) \cdot P_{FO} \right) + c \cdot \left( F_{DF\ FO}\left(S^*_{DF\ FO\ L,B}\right) \cdot P_{FO} \right) + (C_o + C_c) + q \cdot (W \cdot P_C \cdot \frac{r}{365}) \right) + C_{TI} \right]$$

Assuming a fuel consumption function (Equation (2)):

$$F_{DF\ LNG}(s^*, \nabla) = F_{DF\ LNG\ d} \cdot \left( \frac{S^*_{DF\ LNG\ L,B}}{S_d} \right)^a \cdot \left( \frac{P + L}{\nabla} \right)^{2/3}$$

The term $c \cdot \left( F_{DF\ FO}\left(S^*_{DF\ FO\ L,B}\right) \cdot P_{FO} \right)$ is set equal to zero through the binary variable, $c$, whilst the term: $b \cdot F_{DF\ LNG}\left(S^*_{DF\ LNG\ L,B}\right) \cdot P_{LNG}$ is retained, since $b = 1$, when assuming the use of LNG as a fuel. The only decision variable is the speed, $s^*_{DF\ LNG\ L,B}$, with the rest being data inputs to the problem. The pilot fuel oil consumption follows the same exponential relationship between speed and fuel consumption as in the other fuels. This can be explained by the fact that pilot fuel oil consumption is proportional to the engine speed, which in turn is nearly proportional to the ship speed (MAN Energy Solutions 2020). This means that the pilot fuel oil consumption varies nearly linearly with ship speed (MAN Energy Solutions 2020).

By substituting Equation (2) into Equation (7):

$$RFR = \frac{1}{W} \cdot \left[ \left( \frac{D_{SCR,NSR,Cape}}{\left(S^*_{DF\ LNG\ L,B}\right) \cdot 24} \right) \cdot \left( b \cdot \left( F_{DF\ LNG}\left(S^*_{DF\ LNG\ L,B}\right) \cdot P_{LNG} + F_{DF\ Pilot}\left(S^*_{DF\ LNG\ L,B}\right) \cdot P_{FO} \right) + (C_o + C_c) + q \cdot (W \cdot P_C \cdot \frac{r}{365}) \right) + C_{TI} \right]$$

And by expanding:

$$RFR = \frac{D_{SCR,NSR,Cape} \cdot \left( F_{DF\ LNG\ d} \cdot P_{LNG} + F_{DF\ Pilot\ d} \cdot P_{FO} \right) \cdot {S^*_{DF\ LNG\ L,B}}^{(a-1)} \cdot (P + L)^{\frac{2}{3}}}{W \cdot 24 \cdot {S_d}^a \cdot \nabla^{\frac{2}{3}}} + \frac{\left( (C_o + C_c) + q \cdot \left( W \cdot P_C \cdot \frac{r}{365} \right) \right) \cdot D_{SCR,NSR,Cape}}{W \cdot 24} \cdot \frac{1}{S^*_{DF\ LNG\ L,B}} + \frac{C_{TI}}{W}$$

The first order condition to obtain the optimal speed, $S^*_{DF\ LNG\ L,B}$, which minimises the $RFR$ is $\frac{\partial RFR}{\partial S^*_{DF\ LNG\ L,B}} = 0$:

$$\frac{(a-1)\cdot D_{SCR,NSR,Cape}\cdot(F_{DF\ LNG\ d}\cdot P_{LNG}+F_{DF\ Pilot\ d}\cdot P_{FO})\cdot(P+L)^{\frac{2}{3}}}{W\cdot 24\cdot {S_d}^a\cdot\nabla^{\frac{2}{3}}}\cdot {S^*_{DF\ LNG\ L,B}}^{(a-2)} - \frac{\left((C_o+C_c)+q\cdot\left(W\cdot P_C\cdot\frac{r}{365}\right)\right)\cdot D_{SCR,NSR,Cape}}{W\cdot 24}\cdot\frac{1}{{S^*_{DF\ LNG\ L,B}}^2} = 0$$

And by rearranging, the optimal speed, $S^*_{DF\ LNG\ L,B}$ is:

$${S^*_{DF\ LNG\ L,B}}^a = \frac{\left((C_o+C_c)+q\cdot\left(W\cdot P_C\cdot\frac{r}{365}\right)\right)\cdot {S_d}^a\cdot\nabla^{\frac{2}{3}}}{(a-1)\cdot(F_{DF\ LNG\ d}\cdot P_{LNG}+F_{DF\ Pilot\ d}\cdot P_{FO})\cdot(P+L)^{\frac{2}{3}}} \qquad \text{or} \qquad S^*_{DF\ LNG\ L,B} = \sqrt[a]{\frac{\left((C_o+C_c)+q\cdot\left(W\cdot P_C\cdot\frac{r}{365}\right)\right)\cdot {S_d}^a\cdot\nabla^{\frac{2}{3}}}{(a-1)\cdot(F_{DF\ LNG\ d}\cdot P_{LNG}+F_{DF\ Pilot\ d}\cdot P_{FO})\cdot(P+L)^{\frac{2}{3}}}}$$

The second order condition is:

$$\frac{\partial^2 RFR}{\partial {S^*_{DF\ LNG\ L,B}}^2} = \frac{(a-1)\cdot(a-2)\cdot D_{SCR,NSR,Cape}\cdot(F_{DF\ LNG\ d}\cdot P_{LNG}+F_{DF\ Pilot\ d}\cdot P_{FO})\cdot(P+L)^{\frac{2}{3}}}{W\cdot 24\cdot {S_d}^a\cdot\nabla^{\frac{2}{3}}}\cdot {S^*_{DF\ LNG\ L,B}}^{(a-3)} + \frac{2\cdot\left((C_o+C_c)+q\cdot\left(W\cdot P_C\cdot\frac{r}{365}\right)\right)\cdot D_{SCR,NSR,Cape}}{W\cdot 24}$$
$$\cdot\frac{1}{{S^*_{DF\ LNG\ L,B}}^3}$$

For $a = 3$ (cubic fuel consumption function):

$$= \frac{2\cdot D_{SCR,NSR,Cape}\cdot(F_{DF\ LNG\ d}\cdot P_{LNG}+F_{DF\ Pilot\ d}\cdot P_{FO})\cdot(P+L)^{\frac{2}{3}}}{W\cdot 24\cdot {S_d}^3\cdot\nabla^{\frac{2}{3}}} + \frac{2\cdot\left((C_o+C_c)+q\cdot\left(W\cdot P_C\cdot\frac{r}{365}\right)\right)\cdot D_{SCR,NSR,Cape}}{W\cdot 24}\cdot\frac{1}{{S^*_{DF\ LNG\ L,B}}^3}$$

Substituting the data inputs and the value of the optimal speed obtained from the first order condition every time, it is proved that $\frac{\partial^2 RFR}{\partial {S^*_{DF\ LNG\ L,B}}^2} > 0$. Thus the solution is unique and is a global minimum in $\underline{S} \le s^* \le \overline{S}$.

Moreover, the optimal speed when a tanker conducts ballast voyages (Equation (9), the same as above with the term, $q \cdot \left(W \cdot P_C \cdot \frac{r}{365}\right)$, set equal to zero through the binary variable, $q$. The only difference is the notation of speed and fuel consumption.

**Appendix C1.** Port characteristics for LR2 tankers of 115,000 dwt, length overall (LOA) of 250 metres, and loaded draught of 12 metres.

| Port | Tanker Terminals | Berths/Jetties | DWT | LOA (metres) | Draught (metres) |
|---|---|---|---|---|---|
| Ulsan | S-Oil 2-1/Sk Corp Sk8 | 2 | 120,000/150,000 | 250/280 | 13.50/16.50 |
| Rotterdam | 11 terminals/berths for clean oil products | 11 | 120,000 – 355,000 | 270 – 375 | 12.65 – 20.70 |
| Bilbao | Petronor/Punta Lucero No 1, No 2 | 2 | 150,000 – 500,000 | 325 – 400 | 18.50 – 30.00 |
| Chiba | Fuji Oil Pier | 1 | 120,000 | 285 | 14.54 |
| Coryton | Shellhaven Terminal (Stanford-le-Hope) South Jetty | 1 | | 275 | 15.00 |

Source: Refinitiv Eikon (2021).

**Appendix C2**. LNG bunkering infrastructure/ships.

| Port | LNG infrastructure | LNG Tank Capacity ($m^3$) | Country | Operations |
|---|---|---|---|---|
| Ulsan | LNG Bunker Ship SM Jeju LNG2 | 7,654 | South Korea | Coastal in South Korea |
| Rotterdam | LNG Bunker Ship Coral Fraseri (Ice Class II) | 10,000 | The Netherlands | North Sea, Baltic Sea, West Mediterranean |
| | LNG Bunker Ship Coral Methane (Ice Class IB) | 7,551 | The Netherlands | North Sea, Baltic Sea, West Mediterranean |
| | LNG Bunker Ship Coralius (Ice Class IA) | 5,600 | Norway | North Sea, Baltic Sea |
| | LNG Bunker Ship Cardissa | 6,500 | The Netherlands | North Sea, Baltic Sea |
| Rotterdam | GATE Terminal Rotterdam | 720,000 | The Netherlands | Rotterdam |
| | LNG Bunker Barge Flexfueler 001 | 1,480 | The Netherlands | ARA region* |
| | LNG Bunker Barge LNG London | 2,998 | The Netherlands | Rotterdam |
| Bilbao | Bilbao LNG Terminal | 600-270,000 | Spain | Spain |
| | LNG bunker station Bilbao | 1,000 | Spain | Spain |
| Chiba | Yokohama LNG bunkering | 1,180,000 | Japan | Tokyo Bay (Japan) |
| | LNG Bunker Ship Ecobunker Tokyo Bay | 2,500 | Japan | Tokyo Bay (Japan) |
| Coryton | Isle of Grain LNG Terminal | 2,000-1,200,000 | Isle of Grain | UK |

Sources: email communication with Sumitomo, March 2020, DNV (2021), Clarksons (2021). *ARA region: Amsterdam-Rotterdam-Antwerp region.

**Appendix D1.** LNG/VLSFO distance ratios (Authors' calculations).

LNG/VLSFO distance ratio per route alternative and OD pair for the 1,700 $m^3$ mode.

| Route | Chiba – Coryton | Ulsan – Rotterdam | Ulsan – Bilbao |
|---|---|---|---|
| | Ratio | | |
| | Optimal Speed | | |
| Cape | 53/47 | 54/46 | 56/44 |
| SCR | 69/31 | 71/29 | 75/25 |
| NSR | 89/11 | 97/3 | 89/11 |
| | 12 knots | | |
| Cape | 81/19 | 83/17 | 86/14 |
| SCR | 100/0 | 100/0 | 100/0 |
| NSR | 100/0 | 100/0 | 100/0 |

LNG/VLSFO distance ratio per route alternative and OD pair for the 3,600 $m^3$ mode.

| Route | Chiba – Coryton | Ulsan – Rotterdam | Ulsan – Bilbao |
|---|---|---|---|
| | Ratio | | |
| | Optimal Speed | | |
| Cape | 97/3 | 99/1 | 100/0 |
| SCR | 100/0 | 100/0 | 100/0 |
| NSR | 100/0 | 100/0 | 100/0 |
| | 12 knots | | |
| Cape | 100/0 | 100/0 | 100/0 |
| SCR | 100/0 | 100/0 | 100/0 |
| NSR | 100/0 | 100/0 | 100/0 |

**Appendix E1.** Results for HSFO-Scrubber mode.

| ΔRFR | HSFO-Scrubber | | MGO in NSR | | HSFO-Scrubber | | | MGO in NSR | | | HSFO-Scrubber | | | MGO in NSR | | |
|---|---|---|---|---|---|---|---|---|---|---|---|---|---|---|---|---|
| | Low Fuel - Jet/Gasoil Prices – High USD/RUB rate | | | | Base Case | | | | | | High Fuel - Jet/Gasoil Prices – Low USD/RUB rate | | | | | |
| | Official Fees | Independent Navigation | Official Fees | Independent Navigation | Official Fees | Discounted Fees | Independent Navigation | Official Fees | Discounted Fees | Independent Navigation | Official Fees | Discounted Fees | Independent Navigation | Official Fees | Discounted Fees | Independent Navigation |
| | | | | | | | **Chiba – Coryton** | | | | | | | | | |
| | | | | | | | Optimal Speed | | | | | | | | | |
| SCR-NSR | 0.8 | 5.6 | 0.7 | 5.5 | 1.5 | 2.0 | 7.0 | 1.2 | 1.7 | 6.7 | -2.1 | 3.5 | 8.5 | -2.6 | 3.0 | 8.0 |
| | (-2.2) | (2.6) | (-2.3) | (2.4) | (-1.6) | (-1.2) | (3.8) | (-1.9) | (-1.5) | (3.5) | (-5.4) | (0.2) | (5.2) | (-5.9) | (-0.3) | (4.7) |
| Cape-NSR | 0.4 | 5.2 | 0.3 | 5.1 | 2.5 | 3.0 | 8.0 | 2.2 | 2.7 | 7.7 | 0.3 | 5.9 | 10.9 | -0.2 | 5.5 | 10.5 |
| | (-2.6) | (2.2) | (-2.7) | (2.1) | (-0.6) | (-0.1) | (4.9) | (-0.9) | (-0.4) | (4.6) | (-3.0) | (2.6) | (7.6) | (-3.5) | (2.2) | (7.2) |
| SCR-Cape | 0.4 | | 0.4 | | -1.0 | | | -1.0 | | | -2.4 | | | -2.4 | | |
| | | | | | | | 12 knots | | | | | | | | | |
| SCR-NSR | 1.9 | 6.7 | 1.8 | 6.6 | 2.5 | 3.0 | 8.0 | 2.2 | 2.7 | 7.7 | -1.3 | 4.3 | 9.3 | -1.7 | 3.9 | 8.9 |
| | (-1.2) | (3.6) | (-1.3) | (3.5) | (-0.7) | (-0.2) | (4.8) | (-1.0) | (-0.5) | (4.5) | (-4.6) | (1.0) | (6.0) | (-5.1) | (0.6) | (5.6) |
| Cape-NSR | 2.2 | 7.0 | 2.0 | 6.8 | 4.0 | 4.5 | 9.5 | 3.7 | 4.2 | 9.2 | 1.5 | 7.1 | 12.1 | 1.0 | 6.6 | 11.6 |
| | (-0.9) | (3.8) | (-1.1) | (3.7) | (0.8) | (1.3) | (6.3) | (0.5) | (1.0) | (6.0) | (-1.8) | (3.8) | (8.8) | (-2.3) | (3.3) | (8.3) |
| SCR-Cape | -0.2 | | -0.2 | | -1.5 | | | -1.5 | | | -2.8 | | | -2.8 | | |
| | | | | | | | **Ulsan – Rotterdam** | | | | | | | | | |
| | | | | | | | Optimal Speed | | | | | | | | | |
| SCR-NSR | 0.2 | 5.0 | 0.0 | 4.8 | 0.7 | 1.1 | 6.1 | 0.4 | 0.8 | 5.8 | -3.2 | 2.4 | 7.4 | -3.7 | 1.9 | 6.9 |
| | (-2.7) | (2.1) | (-2.9) | (1.9) | (-2.4) | (-1.9) | (3.1) | (-2.7) | (-2.2) | (2.8) | (-6.4) | (-0.8) | (4.2) | (-6.8) | (-1.2) | (3.8) |
| Cape-NSR | -0.2 | 4.6 | -0.4 | 4.4 | 1.7 | 2.2 | 7.2 | 1.4 | 1.8 | 6.8 | -0.8 | 4.8 | 9.8 | -1.3 | 4.4 | 9.4 |
| | (-3.1) | (1.7) | (-3.3) | (1.5) | (-1.4) | (-0.9) | (4.1) | (-1.7) | (-1.2) | (3.8) | (-4.0) | (1.6) | (6.6) | (-4.4) | (1.2) | (6.2) |
| SCR-Cape | 0.4 | | 0.4 | | -1.0 | | | -1.0 | | | -2.4 | | | -2.4 | | |
| | | | | | | | 12 knots | | | | | | | | | |
| SCR-NSR | 1.2 | 6.0 | 1.1 | 5.9 | 1.6 | 2.1 | 7.1 | 1.3 | 1.8 | 6.8 | -2.4 | 3.2 | 8.2 | -2.9 | 2.7 | 7.7 |
| | (-1.8) | (3.0) | (-2.0) | (2.8) | (-1.5) | (-1.0) | (4.0) | (-1.8) | (-1.3) | (3.7) | (-5.6) | (0.0) | (5.0) | (-6.1) | (-0.5) | (4.5) |
| Cape-NSR | 1.4 | 6.2 | 1.3 | 6.1 | 3.1 | 3.6 | 8.6 | 2.8 | 3.3 | 8.3 | 0.3 | 5.9 | 10.9 | -0.1 | 5.5 | 10.5 |
| | (-1.6) | (3.2) | (-1.7) | (3.1) | (0.0) | (0.5) | (5.5) | (-0.3) | (0.2) | (5.2) | (-2.9) | (2.8) | (7.8) | (-3.3) | (2.3) | (7.3) |
| SCR-Cape | -0.2 | | -0.2 | | -1.5 | | | -1.5 | | | -2.8 | | | -2.8 | | |
| | | | | | | | **Ulsan – Bilbao** | | | | | | | | | |
| | | | | | | | Optimal Speed | | | | | | | | | |
| SCR-NSR | -1.3 | 3.5 | -1.5 | 3.3 | -1.4 | -0.9 | 4.1 | -1.7 | -1.2 | 3.8 | -5.8 | -0.2 | 4.8 | -6.2 | -0.6 | 4.4 |
| | (-5.0) | (-0.2) | (-5.1) | (-0.3) | (-5.4) | (-4.9) | (0.1) | (-5.7) | (-5.2) | (-0.2) | (-10.0) | (-4.4) | (0.6) | (-10.5) | (-4.9) | (0.1) |
| Cape-NSR | -1.7 | 3.1 | -1.9 | 2.9 | -0.4 | 0.1 | 5.1 | -0.7 | -0.2 | 4.8 | -3.4 | 2.2 | 7.2 | -3.9 | 1.8 | 6.8 |
| | (-5.4) | (-0.6) | (-5.6) | (-0.8) | (-4.4) | (-3.9) | (1.1) | (-4.7) | (-4.2) | (0.8) | (-7.6) | (-2.0) | (3.0) | (-8.1) | (-2.5) | (2.5) |
| SCR-Cape | 0.4 | | 0.4 | | -1.0 | | | -1.0 | | | -2.4 | | | -2.4 | | |
| | | | | | | | 12 knots | | | | | | | | | |
| SCR-NSR | -0.5 | 4.3 | -0.7 | 4.1 | -0.6 | -0.1 | 4.9 | -0.9 | -0.4 | 4.6 | -5.1 | 0.5 | 5.5 | -5.6 | 0.1 | 5.1 |
| | (-4.4) | (0.4) | (-4.6) | (0.2) | (-4.7) | (-4.2) | (0.8) | (-5.0) | (-4.5) | (0.5) | (-9.4) | (-3.8) | (1.2) | (-9.8) | (-4.2) | (0.8) |
| Cape-NSR | -0.3 | 4.5 | -0.4 | 4.4 | 0.9 | 1.4 | 6.4 | 0.6 | 1.1 | 6.1 | -2.4 | 3.2 | 8.2 | -2.8 | 2.8 | 7.8 |
| | (-4.2) | (0.6) | (-4.4) | (0.4) | (-3.2) | (-2.7) | (2.3) | (-3.5) | (-3.0) | (2.0) | (-6.6) | (-1.0) | (4.0) | (-7.1) | (-1.5) | (3.5) |
| SCR-Cape | -0.2 | | -0.2 | | -1.5 | | | -1.5 | | | -2.7 | | | -2.7 | | |

Note: RFR Differentials in parentheses refer to results when ice damage repairs are factored in the analysis.

**Appendix E1.** Results for VLSFO mode.

| ΔRFR | VLSFO | | MGO in NSR | | VLSFO | | MGO in NSR | | | | VLSFO | | MGO in NSR | | | |
|---|---|---|---|---|---|---|---|---|---|---|---|---|---|---|---|---|
| | Low Fuel - Jet/Gasoil Prices – High USD/RUB rate | | | | Base Case | | | | | | High Fuel - Jet/Gasoil Prices – Low USD/RUB rate | | | | | |
| | Official Fees | Independent Navigation | Official Fees | Independent Navigation | Official Fees | Discounted Fees | Independent Navigation | Official Fees | Discounted Fees | Independent Navigation | Official Fees | Discounted Fees | Independent Navigation | Official Fees | Discounted Fees | Independent Navigation |
| | | | | | | | **Chiba – Coryton** | | | | | | | | | |
| | | | | | | | Optimal Speed | | | | | | | | | |
| SCR-NSR | 1.2 | 6.0 | 1.2 | 6.0 | 2.4 | 2.9 | 7.9 | 2.4 | 2.9 | 7.9 | -1.0 | 4.6 | 9.6 | -1.0 | 4.6 | 9.6 |
| | (-1.9) | (2.9) | (-1.9) | (2.9) | (-0.9) | (-0.4) | (4.6) | (-0.9) | (-0.4) | (4.6) | (-4.4) | (1.2) | (6.2) | (-4.4) | (1.2) | (6.2) |
| Cape-NSR | 1.2 | 6.0 | 1.2 | 6.0 | 4.2 | 4.7 | 9.7 | 4.2 | 4.7 | 9.7 | 2.4 | 8.0 | 13.0 | 2.4 | 8.0 | 13.0 |
| | (-1.9) | (2.9) | (-1.9) | (2.9) | (0.9) | (1.4) | (6.4) | (0.9) | (1.4) | (6.4) | (-1.0) | (4.6) | (9.6) | (-1.1) | (4.6) | (9.6) |
| SCR-Cape | 0.0 | | 0.0 | | -1.7 | | | -1.7 | | | -3.4 | | | -3.4 | | |
| | | | | | | | 12 knots | | | | | | | | | |
| SCR-NSR | 2.0 | 6.8 | 2.0 | 6.8 | 2.8 | 3.3 | 8.3 | 2.8 | 3.3 | 8.3 | -0.8 | 4.8 | 9.8 | -0.8 | 4.8 | 9.8 |
| | (-1.1) | (3.7) | (-1.1) | (3.7) | (-0.5) | (0.0) | (5.0) | (-0.5) | (0.0) | (5.0) | (-4.3) | (1.4) | (6.4) | (-4.3) | (1.4) | (6.4) |
| Cape-NSR | 2.4 | 7.2 | 2.4 | 7.2 | 4.7 | 5.2 | 10.2 | 4.7 | 5.2 | 10.2 | 2.6 | 8.2 | 13.2 | 2.6 | 8.2 | 13.2 |
| | (-0.8) | (4.0) | (-0.8) | (4.0) | (1.4) | (1.9) | (6.9) | (1.4) | (1.9) | (6.9) | (-0.8) | (4.8) | (9.8) | (-0.8) | (4.8) | (9.8) |
| SCR-Cape | -0.4 | | -0.4 | | -1.9 | | | -1.9 | | | -3.4 | | | -3.4 | | |
| | | | | | | | **Ulsan – Rotterdam** | | | | | | | | | |
| | | | | | | | Optimal Speed | | | | | | | | | |
| SCR-NSR | 0.5 | 5.3 | 0.5 | 5.3 | 1.4 | 1.9 | 6.9 | 1.4 | 1.9 | 6.9 | -2.2 | 3.4 | 8.4 | -2.2 | 3.4 | 8.4 |
| | (-2.5) | (2.3) | (-2.5) | (2.3) | (-1.7) | (-1.2) | (3.8) | (-1.7) | (-1.2) | (3.8) | (-5.5) | (0.1) | (5.1) | (-5.5) | (0.1) | (5.1) |
| Cape-NSR | 0.5 | 5.3 | 0.5 | 5.3 | 3.2 | 3.7 | 8.7 | 3.2 | 3.7 | 8.7 | 1.1 | 6.7 | 11.7 | 1.1 | 6.7 | 11.7 |
| | (-2.5) | (2.3) | (-2.5) | (2.3) | (0.0) | (0.5) | (5.5) | (0.0) | (0.5) | (5.5) | (-2.2) | (3.4) | (8.4) | (-2.2) | (3.4) | (8.4) |
| SCR-Cape | 0.0 | | 0.0 | | -1.7 | | | -1.7 | | | -3.4 | | | -3.4 | | |
| | | | | | | | 12 knots | | | | | | | | | |
| SCR-NSR | 1.3 | 6.1 | 1.3 | 6.1 | 1.8 | 2.3 | 7.3 | 1.8 | 2.3 | 7.3 | -2.1 | 3.5 | 8.5 | -2.1 | 3.5 | 8.5 |
| | (-1.8) | (3.0) | (-1.8) | (3.0) | (-1.4) | (-0.9) | (4.1) | (-1.4) | (-0.9) | (4.1) | (-5.4) | (0.2) | (5.2) | (-5.4) | (0.2) | (5.2) |
| Cape-NSR | 1.6 | 6.4 | 1.6 | 6.4 | 3.7 | 4.2 | 9.2 | 3.7 | 4.2 | 9.2 | 1.3 | 7.0 | 12.0 | 1.3 | 6.9 | 11.9 |
| | (-1.4) | (3.4) | (-1.4) | (3.4) | (0.5) | (1.0) | (6.0) | (0.5) | (1.0) | (6.0) | (-2.0) | (3.6) | (8.6) | (-2.0) | (3.6) | (8.6) |
| SCR-Cape | -0.4 | | -0.4 | | -1.9 | | | -1.9 | | | -3.4 | | | -3.4 | | |
| | | | | | | | **Ulsan – Bilbao** | | | | | | | | | |
| | | | | | | | Optimal Speed | | | | | | | | | |
| SCR-NSR | -1.1 | 3.7 | -1.1 | 3.7 | -0.9 | -0.4 | 4.6 | -0.9 | -0.4 | 4.6 | -5.2 | 0.4 | 5.4 | -5.2 | 0.4 | 5.4 |
| | (-5.0) | (-0.2) | (-5.0) | (-0.2) | (-5.1) | (-4.6) | (0.4) | (-5.1) | (-4.6) | (0.4) | (-9.7) | (-4.1) | (0.9) | (-9.7) | (-4.1) | (0.9) |
| Cape-NSR | -1.2 | 3.6 | -1.2 | 3.6 | 0.8 | 1.3 | 6.3 | 0.8 | 1.3 | 6.3 | -1.9 | 3.8 | 8.8 | -1.9 | 3.8 | 8.8 |
| | (-5.0) | (-0.2) | (-5.0) | (-0.2) | (-3.4) | (-2.9) | (2.1) | (-3.4) | (-2.9) | (2.1) | (-6.4) | (-0.7) | (4.3) | (-6.4) | (-0.8) | (4.2) |
| SCR-Cape | 0.0 | | 0.0 | | -1.7 | | | -1.7 | | | -3.3 | | | -3.3 | | |
| | | | | | | | 12 knots | | | | | | | | | |
| SCR-NSR | -0.5 | 4.3 | -0.5 | 4.3 | -0.6 | -0.1 | 4.9 | -0.6 | -0.1 | 4.9 | -5.0 | 0.6 | 5.6 | -5.0 | 0.6 | 5.6 |
| | (-4.5) | (0.3) | (-4.5) | (0.3) | (-4.8) | (-4.3) | (0.7) | (-4.8) | (-4.3) | (0.7) | (-9.5) | (-3.9) | (1.1) | (-9.6) | (-3.9) | (1.1) |
| Cape-NSR | -0.2 | 4.6 | -0.2 | 4.6 | 1.3 | 1.8 | 6.8 | 1.3 | 1.8 | 6.8 | -1.6 | 4.0 | 9.0 | -1.7 | 4.0 | 9.0 |
| | (-4.1) | (0.7) | (-4.1) | (0.7) | (-2.9) | (-2.4) | (2.6) | (-2.9) | (-2.4) | (2.6) | (-6.2) | (-0.6) | (4.4) | (-6.2) | (-0.6) | (4.4) |
| SCR-Cape | -0.4 | | -0.4 | | -1.9 | | | -1.9 | | | -3.4 | | | -3.4 | | |

Note: RFR Differentials in parentheses refer to results when ice damage repairs are factored in the analysis.

**Appendix E1.** Results for LNG-VLSFO mode with tank capacities of 1,700 $m^3$ and 3,600 $m^3$.

| ΔRFR | LNG-VLSFO at 1,700 $m^3$ | | LNG-VLSFO at 3,600 $m^3$ | | LNG-VLSFO at 1,700 $m^3$ | | | LNG-VLSFO at 3,600 $m^3$ | | | LNG-VLSFO at 1,700 $m^3$ | | | LNG-VLSFO at 3,600 $m^3$ | | |
|---|---|---|---|---|---|---|---|---|---|---|---|---|---|---|---|---|
| | Low Fuel - Jet/Gasoil Prices – High USD/RUB rate | | | | Base Case | | | | | | High Fuel - Jet/Gasoil Prices – Low USD/RUB rate | | | | | |
| | Official Fees | Independent Navigation | Official Fees | Independent Navigation | Official Fees | Discounted Fees | Independent Navigation | Official Fees | Discounted Fees | Independent Navigation | Official Fees | Discounted Fees | Independent Navigation | Official Fees | Discounted Fees | Independent Navigation |
| | | | | | | | **Chiba – Coryton** | | | | | | | | | |
| | | | | | | | Optimal Speed | | | | | | | | | |
| SCR-NSR | 1.1 | 5.9 | 0.6 | 5.4 | 2.0 | 2.5 | 7.5 | 1.0 | 1.5 | 6.5 | -1.6 | 4.0 | 9.0 | -3.1 | 2.5 | 7.5 |
| | (-1.9) | (2.9) | (-2.3) | (2.5) | (-1.1) | (-0.6) | (4.4) | (-2.1) | (-1.6) | (3.4) | (-4.8) | (0.8) | (5.8) | (-6.3) | (-0.6) | (4.4) |
| Cape-NSR | 1.2 | 6.0 | 0.2 | 5.0 | 3.9 | 4.3 | 9.3 | 1.8 | 2.2 | 7.2 | 1.9 | 7.5 | 12.5 | -1.2 | 4.4 | 9.4 |
| | (-1.8) | (3.0) | (-2.7) | (2.1) | (0.8) | (1.3) | (6.3) | (-1.3) | (-0.8) | (4.2) | (-1.3) | (4.3) | (9.3) | (-4.4) | (1.3) | (6.3) |
| SCR-Cape | -0.1 | | 0.4 | | -1.9 | | | -0.8 | | | -3.5 | | | -1.9 | | |
| | | | | | | | 12 knots | | | | | | | | | |
| SCR-NSR | 1.9 | 6.7 | 1.9 | 6.7 | 2.3 | 2.8 | 7.8 | 2.3 | 2.8 | 7.8 | -1.7 | 3.9 | 8.9 | -1.7 | 4.0 | 9.0 |
| | (-1.2) | (3.6) | (-1.2) | (3.6) | (-0.8) | (-0.3) | (4.7) | (-0.8) | (-0.3) | (4.7) | (-4.9) | (0.7) | (5.7) | (-4.8) | (0.8) | (5.8) |
| Cape-NSR | 2.3 | 7.0 | 2.1 | 6.9 | 4.2 | 4.6 | 9.6 | 3.6 | 4.1 | 9.1 | 1.6 | 7.2 | 12.2 | 0.7 | 6.3 | 11.3 |
| | (-0.8) | (4.0) | (-1.0) | (3.8) | (1.0) | (1.5) | (6.5) | (0.5) | (1.0) | (6.0) | (-1.6) | (4.0) | (9.0) | (-2.5) | (3.1) | (8.1) |
| SCR-Cape | -0.4 | | - 0.3 | | -1.8 | | | -1.3 | | | -3.3 | | | -2.4 | | |
| | | | | | | | **Ulsan – Rotterdam** | | | | | | | | | |
| | | | | | | | Optimal Speed | | | | | | | | | |
| SCR-NSR | 0.6 | 5.4 | 0.0 | 4.8 | 1.4 | 1.9 | 6.9 | 0.2 | 0.7 | 5.7 | -2.4 | 3.2 | 8.2 | -4.1 | 1.5 | 6.5 |
| | (-2.3) | (2.5) | (-2.9) | (1.9) | (-1.6) | (-1.1) | (3.9) | (-2.8) | (-2.3) | (2.7) | (-5.4) | (0.2) | (5.2) | (-7.1) | (-1.5) | (3.5) |
| Cape-NSR | 0.6 | 5.4 | -0.4 | 4.4 | 3.2 | 3.7 | 8.7 | 0.8 | 1.3 | 6.3 | 1.1 | 6.7 | 11.7 | -2.4 | 3.2 | 8.2 |
| | (-2.2) | (2.6) | (-3.3) | (1.5) | (0.3) | (0.8) | (5.8) | (-2.1) | (-1.7) | (3.3) | (-1.9) | (3.7) | (8.7) | (-5.4) | (0.2) | (5.2) |
| SCR-Cape | -0.1 | | 0.4 | | -1.8 | | | -0.6 | | | -3.5 | | | -1.7 | | |
| | | | | | | | 12 knots | | | | | | | | | |
| SCR-NSR | 1.1 | 5.9 | 1.1 | 5.9 | 1.4 | 1.9 | 6.9 | 1.4 | 1.9 | 6.9 | -2.7 | 2.9 | 7.9 | -2.7 | 2.9 | 7.9 |
| | (-1.9) | (2.9) | (-1.9) | (2.9) | (-1.6) | (-1.1) | (3.9) | (-1.6) | (-1.1) | (3.9) | (-5.8) | (-0.2) | (4.8) | (-5.8) | (-0.2) | (4.8) |
| Cape-NSR | 1.5 | 6.3 | 1.4 | 6.2 | 3.2 | 3.7 | 8.7 | 2.7 | 3.2 | 8.2 | 0.4 | 6.0 | 11.0 | -0.4 | 5.3 | 10.3 |
| | (-1.5) | (3.3) | (-1.6) | (3.2) | (0.1) | (0.6) | (5.6) | (-0.3) | (0.2) | (5.2) | (-2.7) | (3.0) | (8.0) | (-3.4) | (2.2) | (7.2) |
| SCR-Cape | -0.4 | | -0.2 | | -1.8 | | | -1.3 | | | -3.2 | | | -2.4 | | |
| | | | | | | | **Ulsan – Bilbao** | | | | | | | | | |
| | | | | | | | Optimal Speed | | | | | | | | | |
| SCR-NSR | -1.1 | 3.7 | -1.4 | 3.4 | -1.0 | -0.5 | 4.5 | -1.7 | -1.2 | 3.8 | -5.4 | 0.2 | 5.2 | -6.3 | -0.7 | 4.3 |
| | (-4.7) | (0.1) | (-5.0) | (-0.3) | (-4.8) | (-4.3) | (0.7) | (-5.5) | (-5.0) | (0.0) | (-9.3) | (-3.7) | (1.3) | (-10.3) | (-4.7) | (0.3) |
| Cape-NSR | -1.1 | 3.7 | -1.9 | 2.9 | 0.8 | 1.3 | 6.3 | -1.1 | -0.6 | 4.4 | -1.9 | 3.7 | 8.7 | -4.7 | 0.9 | 5.9 |
| | (-4.7) | (0.1) | (-5.5) | (-0.7) | (-2.9) | (-2.4) | (2.6) | (-4.9) | (-4.4) | (0.6) | (-5.9) | (-0.3) | (4.7) | (-8.7) | (-3.1) | (1.9) |
| SCR-Cape | 0.0 | | 0.5 | | -1.8 | | | -0.6 | | | -3.5 | | | -1.6 | | |
| | | | | | | | 12 knots | | | | | | | | | |
| SCR-NSR | -0.5 | 4.3 | -0.6 | 4.2 | -0.6 | -0.1 | 4.9 | -0.7 | -0.2 | 4.8 | -5.2 | 0.4 | 5.4 | -5.2 | 0.4 | 5.4 |
| | (-4.4) | (0.4) | (-4.4) | (0.3) | (-4.6) | (-4.1) | (0.9) | (-4.7) | (-4.2) | (0.8) | (-9.2) | (-3.6) | (1.4) | (-9.3) | (-3.7) | (1.3) |
| Cape-NSR | -0.2 | 4.6 | -0.4 | 4.4 | 1.0 | 1.5 | 6.5 | 0.6 | 1.1 | 6.1 | -2.2 | 3.4 | 8.4 | -2.9 | 2.7 | 7.7 |
| | (-4.1) | (0.7) | (-4.2) | (0.6) | (-3.0) | (-2.5) | (2.5) | (-3.4) | (-2.9) | (2.1) | (-6.3) | (-0.7) | (4.3) | (-6.9) | (-1.3) | (3.7) |
| SCR-Cape | -0.3 | | -0.2 | | -1.6 | | | -1.3 | | | -2.9 | | | -2.3 | | |

Note: RFR Differentials in parentheses refer to results when ice damage repairs are factored in the analysis.

List of Tables:



List of Figures: